8-2015

AN ANALYSIS OF THE DIFFERENTIAL METHYLATION AND EXPRESSION OF IMPRINTED GENES IN M. M. MUSCULUS, M. M. DOMESTICUS, AND THEIR HYBRIDS

Anna P. Rice
annarice.ar@gmail.com

AN ANALYSIS OF THE DIFFERENTIAL METHYLATION AND EXPRESSION OF IMPRINTED GENES IN *M. M. MUSCULUS*, *M. M. DOMESTICUS*, AND THEIR HYBRIDS

By

Anna P. Rice

THESIS

Submitted to
Northern Michigan University
In partial fulfillment of the requirements
For the degree of

MASTER OF SCIENCE

Office of Graduate Education and Research

August 2015

SIGNATURE APPROVAL FORM

Title of Thesis: An Analysis of the Differential Methylation and Expression of Imprinted Genes in *M. m. musculus*, *M. m. domesticus*, and their Hybrids

This thesis by Anna P. Rice is recommended for approval by the student's Thesis Committee and Department Head in the Department of Biology and by the Assistant Provost of Graduate Education and Research.

_____

Committee Chair: Dr. Katherine Teeter Date

_____

First Reader: Dr. Alec Lindsay Date

_____

Second Reader (if required): Dr. John Rebers Date

_____

Department Head: Dr. John Rebers Date

_____

Dr. Brian D. Cherry Date
Assistant Provost of Graduate Education and Research

ABSTRACT

AN ANALYSIS OF THE DIFFERENTIAL METHYLATION AND EXPRESSION OF IMPRINTED GENES IN *M. M. MUSCULUS*, *M. M. DOMESTICUS*, AND THEIR HYBRIDS

By

Anna P. Rice

Epigenetics has been found to have an effect on many aspects of biology. Epigenetics refers to modifications of the double-stranded DNA molecule, which do not change the nucleotide sequence but do affect gene expression. DNA methylation is a type of epigenetic modification. Genomic imprinting is a pattern of gene expression that is primarily achieved through DNA methylation, and it results in the expression of only one allele at a particular locus. In this study, I analyzed the methylation patterns of five imprinted genes in the hybrids of two different lab strains of the house mouse subspecies, *M. m. musculus* and *M. m. domesticus*. To detect methylated DNA, bisulfite modification was performed on the genes of the hybrids and parental species. The genes I examined were *Mcts2*, *Nap1l5*, *Peg10*, *Zac1*, and *Zim2*. The results were compared between the parental and hybrid samples. Two of the hybrid samples yielded disruption in the methylation patterns within at least two genes. Each of the parental samples showed disruption in the methylation patterns. I next analyzed the expression levels of five imprinted genes. Quantitative reverse transcription PCR (qRT-PCR) was performed on the genes of the hybrids and parental samples. The genes I examined were *H19*, *Nap1l5*, *Igf2r*, *Mcts2*, and *Mest*. Differences in the expression levels of each of these genes were observed within the parental and hybrid samples.

ACKNOWLEDGMENTS

I would like to thank my research advisor, Dr. Katherine Teeter, for her advice and support; Dr. Alec Lindsay and Dr. John Rebers, who were members of my thesis committee, for providing valuable discussion and feedback on my topic. I would like to thank Dr. Josh Sharp and Krstin Jacobs for their helpful guidance in completing the microbiological aspects of my experiment (i.e. bacterial cloning) as well as the qRT-PCR portion of my experiment; Dr. Erich Ottem and Rebecca Dangremond for providing me with mouse tissues I used as a control as well as for primer efficiency tests prior to the qRT-PCR portion of my experiment; Dr. Bret Payseur of UW-Madison and Dr. David Kass of Eastern Michigan University for providing me with the remaining tissues I required. I would also like to thank the NMU Biology Department and my funding sources, the Excellence in Education Grant and the Spooner Grant.

This thesis follows the format prescribed by the journal *Cell* (www.cell.com/cell/authors#front) and the Department of Biology.

TABLE OF CONTENTS

LIST OF TABLES

LIST OF FIGURES

LIST OF SYMBOLS OR ABBREVIATIONS

1164: *Mmm* x *Mmd*-female

1172: *Mmd*-female

1175: *Mmd*-male

1185: *Mmm*-male

1205: *Mmm* x *Mmd*-male

1216: *Mmd* x *Mmm*-female

1260: *Mmd* x *Mmm*-male

1400: *Mmm*-female

f, ♀: Female

m, ♂: Male

BLAST: Basic local alignment search tool

cDNA: Complementary deoxyribonucleic acid

CG: Cytosine and guanine dinucleotide

DMD: Differentially methylated domain

DMR: Differentially methylated region

DNMT: DNA methyltransferase

eEF-2: Eukaryotic elongation factor 2

Grb10: Growth factor receptor-bound protein 10

H19: An imprinted maternally expressed transcript (non-protein coding)

HPD: Hybrid placental dysplasia

IDT: Integrated DNA technologies

Igf2r: Insulin-like growth factor 2 receptor

Mcts2: Malignant T cell amplified sequence 2

Mest: Mesoderm specific transcript

M. m. domesticus, Mmd, Dom, D: *Mus musculus domesticus* mouse subspecies

M. m. musculus, Mmm, Mus, M: *Mus musculus musculus* mouse subspecies

Nap1l5: Nucleosome assembly protein 1-like 5

PCR: Polymerase chain reaction

Peg10: Paternally expressed gene 10

qPCR: Real-time PCR

qRT-PCR: Real-time PCR

R1: *Mmd*-♀

R2: *Mmd*-♂

R3: *Mmm*-♀

R4: *Mmm*-♂

R5: *Mmd* x *Mmm*-♂

R6: *Mmm* x *Mmd*-♀

R7: *Mmm* x *Mmd*-♂

R8: Control sample from balb/c and Black57 C57/B6 mouse hybrids

UCSC: University of California, Santa Cruz

WAMIDEX: A web atlas of murine genomic imprinting and differential expression

Zac1: Zinc finger protein 1

Zim2: Zinc finger, imprinted 2

INTRODUCTION

Epigenetics has been found to have an effect on many aspects of biology, and research interest in this area has grown rapidly over the last two decades. Epigenetics refers to modifications of the double-stranded DNA molecule that do not change the nucleotide sequence but do affect gene expression. DNA methylation and histone modifications are forms of epigenetic modifications (Gos, 2013; Das and Singal, 2004). Methylation typically occurs on cytosine bases present within dinucleotides consisting of cytosine and guanine (Das and Singal, 2004). DNA methylation typically causes changes in the structure and grooves of DNA, which leads to alterations in the levels of gene expression (Jones and Takai, 2001).

Genomic imprinting is a pattern of gene expression that is primarily achieved through DNA methylation at a differentially methylated domain (DMD). It causes one copy of a gene to be silenced in a parent-of-origin dependent manner (Reinhart et al., 2006). Genomic silencing results in the expression of only one allele at a particular locus, and this expression pattern causes the genes to be functionally haploid (Ashbrook and Hager, 2013; Reinhart et al., 2006; Tilghman, 1999). The silencing of alleles increases the probability that individuals will develop serious conditions caused by recessive alleles at imprinted genes including certain cancers, Prader-Willi Syndrome, and Beckwith-Wiedermann Syndrome (Morison et al., 2005; Virani et al., 2012).

In this experiment, two different subspecies of house mice, *M. m. musculus* and *M. m. domesticus*, were examined. I analyzed the DNA methylation pattern and the expression levels of imprinted genes in the embryos and adult livers of mouse hybrids.

The methylation patterns and expression levels of the parental organisms were also identified. Eight imprinted genes, which have important functions in growth and development, were examined in these organisms. The eight genes I examined were: *Zac1, Mest, Zim2, Peg10, Mcts2, H19, Igf2r,* and *Nap1l5*. Table 1 lists these genes along with their expression pattern and function (Ch.1). In order to detect alterations in the methylation patterns of hybrids and parental species, the differentially methylated domains of the *Mcts2*, *Nap1l5*, *Peg10*, *Zac1*, and *Zim2* genes were compared after bisulfite modification. This information indicated if DNA methylation has indeed been disrupted between the hybrids and parental species. Quantitative reverse transcription polymerase chain reaction (qRT-PCR) was performed for the *Mcts2*, *Nap1l5, H19, Igf2r*, and *Mest* genes in order to ascertain gene expression levels in hybrids. This information indicated if gene expression had indeed been disrupted between the hybrids and parental species. I analyzed only the methylation patterns within the *Peg10*, *Zac1*, and *Zim2* genes, while I examined only the expression levels within the *H19*, *Igf2r*, and *Mest* genes. Both the methylation and expression patterns were analyzed within the *Mcts2* and *Nap1l5* genes.

CHAPTER ONE: LITERATURE REVIEW

Epigenetics and DNA Methylation Background

The fields of Genetics and Epigenetics are growing rapidly. Epigenetics refers to modifications of the double-stranded DNA molecule that do not change the nucleotide sequence but do affect gene expression (Gos, 2013; Das and Singal, 2004). DNA methylation and histone modifications are forms of epigenetic modifications. DNA methylation is involved in the silencing of gene expression as well as chromosome X inactivation. Such methylation is involved in genomic imprinting and regulates chromatin structure. Modifications of the histone proteins that form DNA nucleosomes can change chromatin structure and can have activating or inhibiting effects on gene expression. Alterations in epigenetic modifications are associated with many diseases including cancers (Gos, 2013; Das and Singal, 2004).

DNA methylation typically occurs on cytosine bases present within dinucleotides consisting of cytosine and guanine (Das and Singal, 2004). Methyl groups are added to the fifth position of the cytosine base. The major groove of the DNA molecule is altered through this process and necessary proteins are thus not able to bind to the DNA molecule to initiate transcription and translation (Jones and Takai, 2001). DNA methylation can be propagated to daughter cells (Tycko and Morison, 2002). Methylation of the cytosine bases is a contributor to germ-line and somatic mutations associated with cancer and diabetes mellitus (Arima et al., 2006; Jones and Takai, 2001). DNA methylation is needed for mammalian development and is established through a DNA methyltransferase enzyme. Methylation patterns are reset during gametogenesis

and can be repressed (Lucifero et al., 2002; Tycko and Morison, 2002). Methylation is complete by the metaphase stage of gametogenesis. With females, methylation patterns are initiated and completed in non-replicating oocytes. However, in males, methylation patterns continue to be acquired as germ cells begin to replicate. After fertilization, part of the genome undergoes demethylation (Lucifero et al., 2002).

Genomic Imprinting Background

Genomic imprinting is a pattern of gene expression where only the allele inherited from the mother or the father is expressed. It is primarily achieved through DNA methylation at a differentially methylated domain (DMD) (Reinhart et al., 2006). DMDs are regions about 1 to 5 kb in size. They are often located near the promoters of imprinted genes, and they control gene expression. Imprinted genes are sometimes found in clusters around DMDs. The presence of repeats within these regions is conserved across mammals (Hutter et al., 2010a, 2010b). Within one allele of an imprinted locus, at least 50% of the CG dinucleotides in these regions are methylated, while in the other allele the CG dinucleotides are not methylated. The allele with the methylated nucleotides is unable to be expressed and is therefore silenced (Choufani et al., 2011; Hutter et al., 2010c; Reinhart et al., 2002, 2006; Tycko and Morison, 2002). Genomic silencing results in the expression of only one allele at a particular locus, and this expression pattern causes the genes to be functionally haploid (Ashbrook and Hager, 2013; Reinhart et al., 2006; Tilghman, 1999). Imprinted genes were first identified in the mid-1980s (Edwards and Ferguson-Smith, 2007; Tycko and Morison, 2002). Approximately 100 to 2000 imprinted mouse genes have been identified (Morison et al., 2005; Renfree et al., 2013; Wang et al., 2008, 2011). DNA methyltransferase establishes

imprinting marks. There are three functional DNA methyltransferases in mammals, Dnmt3a, Dnmt3b, and Dnmt3l. The enzymes Dnmt3a and Dnmt3l are essential for the establishment of imprints (Edwards and Ferguson-Smith, 2007).

Imprinted genes are involved in growth, development, metabolism, and are associated with several diseases (Morison et al., 2005; Reinhart et al., 2006; Tilghman, 1999). It is suggested that imprinted genes regulate maternal nutrient supply during embryonic development (Hutter et al., 2010a). In humans, the silencing of alleles increases the probability that serious conditions caused by recessive alleles, including certain cancers, Prader-Willi Syndrome, and Beckwith-Wiedermann Syndrome, will develop (Morison et al., 2005; Virani et al., 2012).

Genomic imprinting and DNA methylation are associated with conditions and diseases. Relaxation or loss of imprinting could represent a new epigenetic mutational mechanism in carcinogenesis. Loss of heterozygosity within imprinted loci is found within a wide variety of tumors and cancers (Edwards and Ferguson-Smith, 2007; Haig, 2004; Rainier et al., 1993). Loss of methylation is observed within patients with diabetes mellitus and hypermethylation is associated with cancers (Arima et al., 2006; Edwards and Ferguson-Smith, 2007). Hypermethylation is often associated with infertility, and methylation patterns have been found to change in offspring conceived through assisted reproductive technologies (Huntriss et al., 2013; Mayer et al., 2000).

Genomic imprinting has been observed within mammals and plants (Hutter et al., 2010a). Several hypotheses have been proposed to explain the emergence of genomic imprinting in mammals. One hypothesis is the parent-offspring conflict (kinship) hypothesis (Ashbrook and Hager, 2013; Burt and Trivers, 1998; Haig, 2000, 2004;

Tilghman, 1999). This hypothesis was proposed in the 1990s. It posits that mothers evolved genomic imprinting to ensure that sufficient resources were provided to them during development of their offspring despite the negative effects alleles inherited from the fathers might have on the health of the mothers. The hypothesis also posits that fathers evolved genomic imprinting to ensure that sufficient resources were provided to their offspring during development despite the effects alleles inherited from the mothers might have on the distribution of maternal resources. This hypothesis suggests that there are opposite maternal and paternal drives controlling the distribution of maternal resources to each offspring (Ashbrook and Hager, 2013; Haig, 2000, 2004; Tilghman, 1999; Tycko and Morison, 2002). The best support for the kinship theory is the contrasting expression pattern observed within the *Igf2* and *Igf2r* imprinted genes. It is believed that maternal-fetal genomic conflict can be involved in mammalian speciation and can cause rapid divergent evolution (Kropáčková et al., 2015).

Another proposed hypothesis is the coadapatation hypothesis (Ashbrook and Hager, 2013; Renfree et al., 2013; Wolf and Hager, 2006). In this model, genes controlling maternal phenotype may affect the offspring, while genes controlling the offspring may affect maternal interactions. This hypothesis posits that the coadaptation observed between offspring and mother is responsible for imprinting. Genomic imprinting would therefore be important in ensuring proper development and the expression of such genes (Ashbrook and Hager, 2013; Renfree et al., 2013; Wolf and Hager, 2006).

A third proposed hypothesis to explain the development of genomic imprinting is the intralocus sexual conflict hypothesis (Ashbrook and Hager, 2013; Day and

Bonduriansky, 2004). This hypothesis suggests that many sexually selected loci should be controlled through imprinting. The hypothesis posits that paternal traits with high fitness will be passed on to sons, while maternal traits with high fitness will be passed on to daughters. Therefore, genomic imprinting evolved due to selection in males and females at particular loci (Ashbrook and Hager, 2013; Day and Bonduriansky, 2004).

Changes in DNA Methylation and Genomic Imprinting Observed within Mouse Hybrids

Previous studies have shown that disruptions in imprinting and methylation patterns are present in the mouse hybrids of the *Peromyscus* and *Mus* genera. In *P. polionotus – P. maniculatus* hybrids, researchers discovered through imprinting assays a loss of imprinting of several genes normally imprinted in both parental species. The identity of the maternal and paternal parental species also was found to determine the offspring and placenta phenotype. These results along with abnormal X-inactivation explain the inviability of these *Peromyscus* hybrids (del Rio et al., 2000; Vrana et al., 1998). In *M. musculus – M. spretus* hybrids, researchers discovered a loss of imprinting through real-time PCR in the *Peg1* or *Mest* gene, which is normally paternally expressed and is important for growth, as well as in the *Peg3* and *Snrpn* genes through real-time PCR and bisulfite sequencing, which are also normally paternally expressed (Shi et al., 2004, 2005). In *M. musculus – M. caroli* hybrids, researchers have found through hybridization studies that there was loss of methylation in retroelements, such as mVL301 and those on chromosome 10, which are able to move around the genome when methylation is lost and affect gene expression (Brown et al., 2008, 2012). Through

bisulfite DNA methylation analyses, the promoters of *Oct4* and *Nanog* genes were found to be demethylated in *M. musculus – M. caroli* hybrids (Battulin et al., 2009).

Speciation and Reproductive Isolation

Reproductive isolation consists of prezygotic and postzygotic stages, and these stages or barriers lead to reproductive barriers. There are several mechanisms of these reproductive barriers. These mechanisms include mate preference, habitat specialization, and spawning synchrony (Palumbi, 1994). When genetic differences between the evolving lineages accumulate, reproductive barriers are created. Reproductive isolation is required for speciation to occur (Palumbi, 1994). Prezygotic barriers include reduced sperm number, defects in sperm form or function, and decreased competitive ability (Turner et al., 2012). Such barriers are not sufficient to cause reproductive isolation (Good et al., 2008a; Turner et al., 2012). Postzygotic reproductive barriers involve hybrid sterility and often involve the X chromosome. The X chromosome in mice includes loci involved in reproductive isolation (Good et al., 2008a; Janoušek et al., 2012). The genetic basis of hybrid sterility is considered complex (Good et al., 2008a, 2008b; Turner et al., 2012). Hybrid placental dysplasia (HPD) is another postzygotic barrier and is associated with increased or decreased placental and fetal growth within hybrids of *Mus musculus* females and *Mus spretus*, *Mus macdonicus*, or *Mus spicilegus* males. It is believed that epigenetic modification of the X chromosome might be the mechanism behind HPD; however, HPD does not occur in the progeny of crosses between *Mmm* and *Mmd*. This suggests that hybrid sterility and HPD evolved independently (Kropáčková et al., 2015).

Genetic differences between populations can be created through a number of events or occasions. Absolute physical barriers such as oceans or long distance can create genetic differences (Geraldes et al., 2011; Palumbi, 1994). Gene flow between populations can be reduced due to the fitness of certain alleles, which can contribute to reproductive isolation (Geraldes et al., 2011). Selection can shape the distribution of variation across groups of organisms. Imprinted genes might react differently under natural selection as compared to biallelically-expressed genes, potentially leading to genetic differences and reproductive isolation and speciation (Geraldes et al., 2011; Hutter et al., 2010a).

The linkage between genetic variation and reproductive isolation is not fully understood within the separate subspecies *M. m. musculus* and *M. m. domesticus* (Geraldes et al., 2011; Good et al., 2008a; Turner et al., 2012). However, it is known that the accumulation of genetic differences can lead to reproductive isolation. Genetic differences leading to reproductive isolation have been observed within genes involved in gamete production, development, and mate recognition (Palumbi, 1994). Most imprinted genes are associated with development (Gregg et al., 2010; Hutter et al., 2010b, 2010c). Some studies suggest that the *Prdm9*, *Hstx1*, and *HS* loci are involved in creating hybrid sterility and speciation of the house mouse subspecies (Bhattacharyya et al., 2013; Flachs et al., 2012, 2014; Mihola et al., 2009). Many genetic differences and genetic incompatibilities are believed to contribute to the hybrid sterility and reproductive isolation of the house mouse (Good et al., 2008a, 2008b; Turner et al., 2012). A single locus, *GA19777*, was found to create reproductive isolation within *Drosophila*

pseudoobscura pseudoobscura and *Drosophila pseudoobscura bogotana* subspecies (Oka et al., 2007; Phadnis and Orr, 2009).

***Mus musculus musculus* and *Mus musculus domesticus* Subspecies**

In this experiment, two different subspecies of the house mouse, *M. m. musculus* and *M. m. domesticus*, were examined. These two subspecies diverged from a common ancestor in the Middle East 350,000 to 500,000 years ago (Geraldes et al., 2011; Janoušek et al., 2012; Kropáčková et al., 2015). They met again at a secondary contact near a narrow hybrid zone in Europe (Geraldes et al., 2011; Janoušek et al., 2012; Kropáčková et al., 2015; Rajabi-Maham et al., 2008). Hybrid zones are considered to be a narrow region where two diverse populations meet and interact, and they are maintained through selection against hybrids. Hybrid zones offer an excellent tool in order to study gene flow and to study the role of various genomic regions in forming reproductive barriers (Božíková et al., 2005; Turner et al., 2012). The hybrid zone of these two populations extends from Bulgaria to Denmark. Hybrids can also be found in Norway (Jones et al., 2010). Research has identified regions of the X chromosome as well as the *Hstl*/*Prdm9* loci as important regions harboring loci involved in creating reproductive isolation between these two genetically distinct populations (Bhattacharyya et al., 2013; Flachs et al., 2012, 2014; Janoušek et al., 2012; Mihola et al., 2009). Hybrid sterility and reproductive isolation of the house mouse is believed to be caused by a complex network of genetic factors (Good et al., 2008a, 2008b; Turner et al., 2012). Hybrid sterility has been proposed to contribute to hybrid failure and thus reproductive isolation (Janoušek et al., 2012; Kropáčková et al., 2015).

Hybrid placental dysplasia (HPD), or increased or decreased placental and fetal growth in interspecific crosses, constitutes a reproductive barrier. *Peromyscus polionotus* and *Peromyscus maniculatus* hybrids experienced disruptions in embryonic and placental growth (Vrana et al., 1998, 2000). HPD is best-studied within the *Mus* genus; however, it does not occur in crosses between *Mmm* and *Mmd* (Janoušek et al., 2012; Kropáčková et al., 2015). It is suggested that DNA methylation is not a feature of HPD (Schütt et al., 2003).

Function and Location of Examined Imprinted Genes

Imprinted genes are important in growth and development. These genes are suggested to control maternal nutrient supply and are often involved in development and metabolism (Morison et al., 2005; Reinhart et al., 2006; Hutter et al., 2010a). Around 100 to 2000 imprinted genes have been identified within the mouse genome (Morison et al., 2005; Renfree et al., 2013; Wang et al., 2008, 2011). Within this experiment, the methylation patterns and then the expression levels of multiple genes were attempted to be tested. A number of primer sets did not successfully amplify the templates (Table 15 and Table 16). A total of eight imprinted genes were actually able to be examined in this experiment. These genes were *H19, Igf2r, Mcts2, Mest, Nap1l5, Peg10, Zac1,* and *Zim2* (Table 1).

The imprinted gene *H19* is expressed within the blastocyst but is repressed after birth. This gene is located on chromosome 7 of the mouse (Bartolomei et al., 1991; Ferguson-Smith et al., 1993). Methylation of the *H19* paternal promoter occurs after fertilization. This gene's imprinting status is conserved across rodents and humans (Bartolomei et al., 1991; Ferguson-Smith et al., 1993). This gene has an important role in

the development of the mouse, and it encodes one of the most abundant RNAs in the developing mouse embryo. The *H19* gene does not encode a protein (Bartolomei et al., 1991; Ferguson-Smith et al., 1993). Within humans, the transcription product of the *H19* gene functions as RNA, and overexpression of this gene is associated with bladder cancer and choriocarcinoma (Brannan et al., 1990; Gregg et al., 2010; Rachmilewitz et al., 1992; Reis et al., 2013).

The *Igf2r* (*Insulin-like growth factor 2 receptor*) gene is located on chromosome 17 of the mouse genome (Birger et al., 1999; Wutz et al., 1997). The gene is expressed from the maternal allele beginning 6.5 days after fertilization. This gene's imprinting status is conserved across mammals (Birger et al., 1999; Wutz et al., 1997; Xu et al., 1993). The mouse *Igf2r* gene contains two DMRs. DMR2 is a target for de novo methylation and is the primary imprinting mark established within the gametes. DMR1 is not independently associated with imprinting. The *Igf2r* gene encodes the insulin-like growth factor type-2 receptor, which is important in growth and development (Birger et al., 1999; Wutz et al., 1997). In humans, the *Igf2r* gene is imprinted in only a small portion of humans, and it encodes a receptor that binds lysosomal enzymes (Xu et al., 1993).

The *Mcts2* (*Malignant T cell amplified sequence 2*) gene is located on chromosome 2 of the mouse genome (Huang et al., 2014). The gene is expressed from the paternal allele only and thus methylated on the maternal allele. This gene's imprinting status is conserved across rodents and humans (Huang et al., 2014; Wood et al., 2007). The *Mcts2* gene contains a domain involved in RNA binding, cell proliferation, and T-cell function (Huang et al., 2014; Wood et al., 2007). Within

humans, this gene is also detected within several forms of cancers (Huang et al., 2014; Wood et al., 2007).

The imprinted *Mest* (*Mesoderm specific transcript*) gene is located on chromosome 6 of the mouse genome (Nishita et al., 1999; Rajabpour-Niknam et al., 2013). This gene is methylated on the maternal allele and is thus expressed from the paternal allele only. This gene's imprinting status is conserved across mammals (Mayer et al., 2010; Nishita et al., 1999; Rajabpour-Niknam et al., 2013). Within mice, the *Mest* gene is expressed within the mesodermal derivatives of the embryo and is turned off within adult tissues. This gene encodes a hydrolase enzyme and regulates placental and fetal growth (Nishita et al., 1999; Rajabpour-Niknam et al., 2013). Within humans, aberrant DNA methylation of the *Mest* gene is associated with female and male infertility, and this gene is expressed during angiogenesis (Huntriss et al., 2013; Mayer et al., 2000).

The imprinted *Nap1l5* (*Nucleosome assembly protein 1-like 5*) gene is located on the sixth chromosome of the mouse genome. This gene is methylated on the maternal allele and is therefore expressed from the paternal allele only (Cowley et al., 2012; Gu et al., 2011). The *Nap1l5* gene encodes the nucleosome assembly protein 1-like 5. The protein encoded by this gene is involved in transcriptional activation and mitotic events, and it is involved in liver cancer (Gu et al., 2011). It has been observed that the function and imprinting status of this gene is conserved within mammals (Cowley et al., 2012; Gu et al., 2011). Within humans, *Nap1l5* is associated with hepatoblastoma, and other such nucleosome assembly proteins have been found to be associated with histone chaperones (Harada et al., 2002).

The imprinted *Peg10* (*Paternally expressed gene 10*) gene is derived from a retrotransposon that integrated into the mammalian genome. This gene is located on the sixth chromosome of the mouse genome (Hishida et al., 2007; Ono et al., 2001). The *Peg10* gene is methylated on the maternal allele and is thus expressed from the paternal allele only. This gene's imprinting status is conserved across mammals (Hishida et al., 2007; Ono et al., 2001). The *Peg10* gene is involved in gene regulation. The *Peg10* region is also involved in the Silver-Russell Syndrome and choriocarcinoma (Hishida et al., 2007; Ono et al., 2001). Within humans, this gene affects cell cycle progression and apoptosis (Hino et al., 2006; Ono et al., 2001).

The imprinted *Zac1* (*Zinc finger protein 1*) gene is located on the tenth chromosome of the mouse genome (Du et al., 2012; Varrault et al., 2006). This gene is methylated on the maternal allele and is therefore expressed from the paternal allele only. This gene's imprinting status is conserved across mammals (Du et al., 2012; Varrault et al., 2006). *Zac1* encodes a zinc finger transcription factor, which induces apoptosis and cell-cycle arrest. This gene is thus involved in controlling embryonic growth as well as intrauterine grown and bone formation (Du et al., 2012; Varrault et al., 2006). Within humans, the *Zac1* gene is associated with neonatal diabetes mellitus, and it serves as a coregulator for nuclear receptors (Daniel et al., 2015).

The imprinted *Zim2* (*Zinc finger, imprinted 2*) gene is located on the seventh chromosome of the mouse genome (Kim et al., 2004). This gene is expressed from the maternal allele only and is methylated within the paternal allele. The imprinting status of the *Zim2* gene is not conserved across mammals and little is known about its function (Kim et al., 2004). This gene does encode a zinc-finger protein (Kim et al., 2004). In

humans, the *Zim2* gene is expressed primarily from the paternal allele, and it serves as a transcription factor (Kim et al., 2000, 2004).

DNA methylation and genomic imprinting are interesting areas of study. Genes that are genomically imprinted are involved in growth, development, metabolism, and allocation of maternal nutrients (Hutter et al., 2010a; Morison et al., 2005; Reinhart et al., 2006). These genes are expressed at key times and ensure embryos survive and develop properly. Disruption in the expression and imprinting patterns of these genes are observed within mouse hybrids and often explain the hybrid inviability and speciation of the organisms involved (Janoušek et al., 2012; Kropáčková et al., 2015; Morison et al., 2005; Reinhart et al., 2006). This study, by examining imprinted genes, helps determine the evolution and speciation of *M. m. musculus* and *M. m. domesticus* subspecies. The conclusions of these experiments could have implications for humans, since many of the genes studied are shared with humans (Morison et al., 2005). Within humans, changes in the DNA methylation pattern of the *Mest* gene are associated with female and male infertility (Huntriss et al., 2013; Mayer et al., 2000). The subspecies of mice used in this study are commonly used in laboratory experiments, thus the study will inform the scientific community about the genomes of these animals as well (Hagan et al., 2004; Shi et al., 2004, 2005).

Table 1. **Description of Genes**. Genes that were examined in this experiment. The chromosome location and gene position were found within the UCSC Genome Browser under Build 37 (Kent et al., 2002).

Gene	Chromosome Location and Position of Gene Transcript (bp)	Maternal or Paternal Expression in the Embryo	Location of Expression	Function	Reference
H19	Chromosome 7; 149661584 – 149861732	Maternally Expressed	Embryo, Placenta, Trophoblast, and Yolk Sac	Has various roles in cancer development	Shoshani et al., 2012
Igf2r	Chromosome 17; 12875272 – 12962572	Maternally Expressed	Embryo, Telencephalon, Cerebrum, Placenta, Liver, and Oocyte	Leads to a receptor for a growth factor important in development	Wutz et al., 1998
Mcts2	Chromosome 2; 152512884 – 152513678	Paternally Expressed	Embryo, Brain, Testes, and Oocyte	Involved in T cell function	Wood et al., 2007
Mest	Chromosome 6; 30688063 – 30698457	Paternally Expressed	Embryo, Placenta, Yolk Sac, Colon, Heart, Liver, Lung, and Oocyte	Leads to a hydrolase linked to certain types of cancer	Ineson et al., 2012
Nap1l5	Chromosome 6; 58855227 – 58857120	Paternally Expressed	Adrenal Gland, Brain, Kidney,	Leads to a nucleosome assembly protein	Cowley et al., 2012

			Oocytes, and Sperm	important in DNA packaging	
Peg10	Chromosome 6; 4697306 – 4710516	Paternally Expressed	Embryo, Placenta, Yolk Sac, and Brain	Important in parthenogenetic development	Hishida et al., 2007
Zac1	Chromosome 10; 12810591 – 12851501	Paternally Expressed	Embryo, Brain, Gut, Heart, Kidney, Liver, Lung, Muscle, Tongue, and Oocyte	Leads to a zinc finger protein that acts as a tumor suppressor	Du et al., 2012
Zim2	Chromosome 7; 6604459 – 6615079	Maternally Expressed	Embryo, Brain, and Testes	Encodes a zinc finger protein and its imprinting status is not conserved among mammals	Kim et al., 2004

CHAPTER TWO: DNA METHYLATION OF IMPRINTED GENES IN MOUSE HYBRIDS

Introduction

DNA methylation is a form of epigenetic modification and typically occurs within mammals and plants. It results in the addition of a methyl group on a cytosine nucleotide (Gos, 2013; Das and Singal, 2004). The methyl group is often added through the activity of a DNA methyltransferase enzyme (Jones and Takai, 2001; Gos, 2013). The DNA of an organism's primordial germ cells typically loses methylation obtained in the previous generation, and then methylation is regained during gametogenesis (Tilghman, 1999). Studies have shown methylation changes within human patients diagnosed with diabetes and cancers (Arima et al., 2006; Rainier et al., 1993). Within humans, the DNA methylation patterns of the *Mest* gene have been found to be associated with infertility (Huntriss et al., 2013; Mayer et al., 2000).

Methylation typically occurs on cytosine bases present within dinucleotides consisting of cytosine and guanine (Das and Singal, 2004). Methylation can cause changes in the structure and grooves of DNA, which often alters the level of gene expression as enzymes and other cofactors cannot bind to the DNA (Jones and Takai, 2001). This change in expression is usually observed when methylation takes place within a portion of the DNA called the differentially methylated domain (DMD) (Reinhart et al., 2006). DMDs are usually 1 to 5 kb in size and contain important structural components that are conserved across mammals (Reinhart et al., 2002, 2006; Paoloni-Giacobino, 2007).

Genomic imprinting is a pattern of gene expression in which only one allele is expressed. It is primarily achieved through DNA methylation at a DMD (Reinhart et al., 2006). With this pattern, one allele at a particular locus typically experiences DNA methylation, which causes it to be silenced and no longer expressed. This genomic silencing results in the expression of only one allele at that particular locus. Genomic imprinting is hypothesized to be important for the growth and development of mammals (Ashbrook and Hager, 2013; Reinhart et al., 2006; Tilghman, 1999).

In this experiment, I compared the DNA methylation pattern of imprinted genes within mouse hybrids to that of their parents. Disruptions of both genomic imprinting and DNA methylation have been found to be present in mouse hybrids (Vrana et al., 1998, 2000). Previous studies have shown that the promoters of *Oct4* and *Nanog* genes were demethylated in *M. musculus-M. caroli* hybrids (Battulin et al., 2009). In *M. musculus-M. spretus* hybrids, researchers discovered a loss of imprinting in the *Peg1* or *Mest*, *Peg3*, and *Snrpn* genes (Shi et al., 2004, 2005). Studies have even shown methylation changes within human patients diagnosed with diabetes and cancers.

I performed bisulfite modification of DNA for this experiment. Bisulfite modification converts any unmethylated cytosines to thymines. The cytosines that remain are therefore methylated. By identifying and comparing the cytosine sites within the DMDs of the samples, this process allowed me to determine if there was any disruption in methylation within the hybrids as compared to the parental species (Sun et al., 2013). Normally, within DMDs, one allele is methylated while the other allele is not methylated. If the hybrids showed a decrease in methylation, I expected to see both alleles containing TGs at CG sites. If the hybrids yielded an increase in methylation, I

expected to see both alleles containing CGs at CG sites. If the methylation pattern within the hybrids was maintained, I expected to see one allele with CGs and the other allele with TGs at the CG sites.

Materials and Methods

The samples that were obtained were *Mmm* x *Mmd*-♀ (1164), *Mmd*-♀ (1172), *Mmd*-♂ (1175), *Mmm*-♂ (1185), *Mmm* x *Mmd*-♂ (1205), *Mmd* x *Mmm*-♀ (1216), *Mmd* x *Mmm*-♂ (1260), and *Mmm*-♀ (1400). The female parents are listed first in the hybrid notation. One male and one female of the two parental samples and one male and one female of the two hybrid samples were obtained. The *Mmd* samples were of the WSB strain, while the *Mmm* samples were of the PWD strain. Mouse livers from these adult samples were obtained from Dr. Bret Payseur of UW-Madison. DNA was previously extracted from these samples through a Qiagen kit.

Zymo Research's EZ DNA Methylation Kit was used to bisulfite-modify the DNA. This kit converts all unmethylated cytosines to uracil. The cytosines that remain in the samples are therefore considered methylated. Using the modified DNA, PCR reactions using a thermocycler were performed to amplify a 300-500 bp portion of the DMDs of five imprinted genes of interest. The five genes of interest were *Mcts2*, *Nap1l5*, *Peg10*, *Zac1*, and *Zim2* (Table 1). A ZymoTaq Premix was used to perform these reactions, and the primers utilized in these reactions were previously physically obtained from IDT (Table 12). The DMDs and primer sequences were identified through the WAMIDEX website (Schulz et al., 2008). A number of primers did not successfully amplify the template (Table 15). I had to initially perform a 10 minute denaturation step

while using this Taq. The PCR products were then purified through gel extractions via the QIAquick® Gel Extraction Kit.

Gel extractions of the PCR products were cloned through Life Technology's TOPO® TA Cloning Kit (Invitrogen). I cloned the PCR products in order to separately examine the alleles of each sample. Using this kit, DNA was ligated to a vector, and then *E. coli* cells were transformed with the vector. The *E. coli* cells were then plated on plates containing 0.5 µg/µl Ampicillin and LB Agar. For each gene, five clones of each sample underwent PCR with the M13 primers to amplify the vector's insert (Table 12). GoTaq (Promega) was used to perform these reactions, and a 10 minute initial denaturation step was used. The PCR products of the clones were purified through gel extractions, and the purified products were then sent to GeneWiz in New Jersey to be sequenced with the M13 primers. I also sequenced the purified, bisulfite-modified DNA for the samples and genes (*Mmd*-♀)-*Nap1l5*, (*Mmm* x *Mmd*-♂)-*Nap1l5*, (*Mmd* x *Mmm*-♀)-*Zim2*, (*Mmd* x *Mmm*-♂)-*Zim2*, (*Mmm*-♀)-*Zim2*, (*Mmm*-♂)-*Mcts2*, (*Mmm* x *Mmd*-♂)-*Mcts2*, (*Mmd* x *Mmm*-♀)-*Mcts2*, (*Mmd* x *Mmm*-♂)-*Mcts2*, and (*Mmd*-♀)-*Zac1* to determine if there was one methylated allele and one unmethylated allele.

The PCR products were sequenced in the forward and reverse directions. The reverse sequences were reverse complemented, so they were identical to the forward sequences. All sequences were reviewed through the Geneious 7 and Mega 6 programs (Kearse et al., 2012; Tamura et al., 2013). Sequences for each gene were input into BLAST to ensure the correct sequence had been amplified (Altschul et al., 1990). The primers were identified and removed from these sequences. Each CG and non-CG site

that experienced methylation in at least one allele of a sample was identified and compared across the samples.

Results

Mcts2 Gene

A 310 bp segment of the DMD of the *Mcts2* gene was sequenced from bisulfite-modified DNA. This DMD region is located within an intron of the *H13* gene and an exon of *Mcts2*. Two clones for the samples *Mmm*-♂, *Mmd* x *Mmm*-♂, and *Mmm* x *Mmd*-♂; three clones for sample *Mmm*-♀; four clones for sample *Mmm* x *Mmd*-♀; and five clones for samples *Mmd*-♀, *Mmd*-♂, and *Mmd* x *Mmm*-♀ were sequenced. The sequences produced were of good quality. I examined 30 CG sites, of which 25/30 showed methylation on only one allele within each sample, and 5/30 showed no methylation on either allele within at least one sample. The parental sample *Mmd*-♀ had 3 CG sites with only TG while sample *Mmd*-♂ had two sites with only TG, and the remaining 27 and 28 respective CG sites had CG and TG (Table 2). The parental sample *Mmm*-♂ had CG and TG at two sites and TG at the remaining 28 available CG sites. The parental sample *Mmm*-♀ had TG at one site and CG and TG at the remaining 29 available sites. The hybrid sample *Mmm* x *Mmd*-♀ had only TG at 1 site and CG and TG at the remaining available 29 sites, while *Mmd* x *Mmm*-♂ had TG at each of the available 30 CG sites. Hybrid sample *Mmm* x *Mmd*-♂ had CG and TG at two sites and TG at 28 sites while *Mmd* x *Mmm*-♀ had CG and TG at 3 sites and TG at the remaining available 27 sites. The *Mmd* x *Mmm*-♀ sample did show partial methylation on both alleles. The discrepancy between the alleles was observed at two sites (Table 2). When the amplified bisulfite-modified DNA was sequenced without being cloned, each of the available sites

had CG and TG for the samples *Mmm*-♂, *Mmm* x *Mmd*-♂, *Mmd* x *Mmm*-♀, and *Mmd* x *Mmm*-♂ (Table 3). In terms of the 3 non-CG sites examined, most samples for most sites had T (Table 2 and Table 3). However, *Mmm* x *Mmd*-♀ had C and T at site 33; *Mmd*-♀ had C and T at site 33; *Mmd*-♂ had C and T at sites 31 and 33; *Mmm*-♂ had C and T at site 32 and C at site 33; *Mmm* x *Mmd*-♂ had C and T at site 33; *Mmd* x *Mmm*-♀ had C and T at site 32 and C at site 33; *Mmd* x *Mmm*-♂ had C and T at site 32 and C at site 33; and *Mmm*-♀ had C and T at sites 32 and 33 (Table 2 and Table 3).

Nap1l5 Gene

A 234 bp segment of the DMD of the *Nap1l5* gene was sequenced from bisulfite-modified DNA. This DMD region is located within an exon and intron of the *Nap1l5* gene and an intron of *Herc3*. Five clones for each sample were sequenced. The sequences produced were of good quality. I examined 22 CG sites, of which 7/22 showed methylation on only one allele within each sample, and 15/22 showed disruption in methylation within at least one sample. The parental sample *Mmd*-♀ had CG and TG at each of the 22 CG sites examined, while sample *Mmd*-♂ had CG and TG at each site except one site with only CG. The *Mmd*-♀ sample yielded partial methylation on both alleles (Table 4). The parental samples *Mmm*-♂ and *Mmm*-♀ had 9 sites with CG and 13 sites with CG and TG. The hybrid sample *Mmd* x *Mmm*-♂ had CG and TG at each of the 22 CG sites. The hybrid sample *Mmm* x *Mmd*-♀ had CG at 11 sites and CG and TG at 11 sites, while *Mmd* x *Mmm*-♀ had TG at 2 sites and CG and TG at the remaining sites (Table 4). According to table 4, sample *Mmm* x *Mmd*-♂ had only CG at 14 sites; however, when the amplified bisulfite-modified DNA was sequenced without being cloned, each of the available sites had CG and TG (Table 5). Table 5 also affirmed that

hybrid sample *Mmd*-♀ had CG and TG at each site. In terms of non-CG sites, every sample had a T at these sites except *Mmd*-♀, which had C and T at site 23; *Mmm* x *Mmd*-♂, which had C and T at sites 24-26; *Mmd* x *Mmm*-♂, which had C and T at site 25; and *Mmm*-♀, which had C and T at site 26 (Table 4 and Table 5).

***Peg10* Gene**

A 228 bp segment of the DMD of the *Peg10* gene was sequenced from bisulfite-modified DNA. This DMD region is located within an exon of the *Peg10* gene. Three clones for sample *Mmm*-♀; four clones for sample *Mmd* x *Mmm*-♂; and five clones for samples *Mmd*-♀, *Mmd*-♂, *Mmm*-♂, *Mmd* x *Mmm*-♀, *Mmm* x *Mmd*-♀, and *Mmm* x *Mmd*-♂ were sequenced. The sequences produced were of good quality. I examined 22 CG sites, and each sample except *Mmm*-♀ experienced methylation on only one allele within each site. Sample *Mmm*-♀ showed methylation on both alleles for 21/22 CG sites and methylation on only one allele for 1/22 site. All of the parental samples except *Mmm*-♀ had CG and TG at each of the 22 CG sites examined (Table 6). The sample *Mmm*-♀ had CG and TG at one site and CG at the remaining 21 sites. All of the hybrid samples had CG and TG at each of the 22 sites (Table 6). In terms of non-CG sites, at site 23 and 25, each sample had C and T. At site 24, sample *Mmm*-♂ had T, while the other samples had C and T. At site 30, sample *Mmm*-♀ had C, while the other samples had C and T. At the sites 26-29, all samples had T except one sample for each site had C and T (Table 6).

***Zac1* Gene**

A 254 bp segment of the DMD of the *Zac1* gene was sequenced from bisulfite-modified DNA. This DMD region is located within an intron of the *Zac1* gene. Two

clones for sample *Mmd*-♀; three clones for sample *Mmm* x *Mmd*-♀; four clones for samples *Mmm*-♀, *Mmd* x *Mmm*-♀, and *Mmm* x *Mmd*-♂; and five clones for samples *Mmd*-♂, *Mmm*-♂, and *Mmd* x *Mmm*-♂ were sequenced. The sequences produced were of good quality. I examined 15 CG sites, of which 7/15 showed methylation on only one allele within each sample, and 8/15 showed no methylation on either allele within at least one sample. All of the parents except *Mmd*-♀ had CG and TG at each of the 15 CG sites examined (Table 7). The hybrid *Mmm* x *Mmd*-♀ had 7 sites with TG and 8 sites with CG and TG, while the hybrid *Mmd* x *Mmm*-♀ had two sites with TG and 13 sites with CG and TG. The *Mmm* x *Mmd*-♀ sample showed partial methylation on both alleles. The discrepancy between the alleles was observed on only one site. The hybrids *Mmm* x *Mmd*-♂ and *Mmd* x *Mmm*-♂ had CG and TG at each of the sites (Table 7). According to Table 7, *Mmd*-♀ had only TG at each of the 15 CG sites; however, when the amplified, bisulfite-modified DNA was sequenced without being cloned, each of the available sites had CG and TG (Table 8). In terms of non-CG sites, every sample had T except *Mmd*-♂, which had C and T at site 18, *Mmm* x *Mmd*-♂, which had C and T at site 17, and *Mmd* x *Mmm*-♀, which had C and T at site 16 (Table 7 and Table 8).

***Zim2* Gene**

A 278 bp segment of the DMD of the *Zim2* gene was sequenced from bisulfite-modified DNA. This DMD region is located within an intron and exon of the *Peg3* gene. Two clones for samples *Mmd*-♀, *Mmd* x *Mmm*-♂, and *Mmm* x *Mmd*-♂; three clones for sample *Mmm*-♀; four clones for sample *Mmm*-♂; five clones for samples *Mmd*-♂ and *Mmm* x *Mmd*-♀; and seven clones for sample *Mmd* x *Mmm*-♀. The sequences produced were of good quality. I examined 21 CG sites, of which 11/21 showed methylation on

only one allele within each sample, and 10/21 showed methylation on both alleles within at least one sample. The parental samples *Mmd*-♂ and *Mmm*-♂ had CG and TG at each of the 21 CG sites examined (Table 9). The parental sample *Mmd*-♀ had 10 sites with CG and 11 sites with CG and TG, while sample *Mmm*-♀ had two sites with CG and TG and 19 sites with CG. The hybrid sample *Mmm* x *Mmd*-♀ had CG and TG at each of the 21 CG sites examined. The hybrid samples *Mmm* x *Mmd*-♂, *Mmd* x *Mmm*-♀, and *Mmd* x *Mmm*-♂ had CG and TG at each of the available 21 sites (Table 9). When the amplified, bisulfite-modified DNA was sequenced without being cloned, the samples *Mmd* x *Mmm*-♀, *Mmd* x *Mmm*-♂, and *Mmm*-♀ had CG and TG at each of the available sites (Table 10). In terms of the 7 non-CG sites examined, most samples for most sites had T (Table 9 and Table 10). However, *Mmm* x *Mmd*-♀ had C and T for 3 sites and C at one site; *Mmd*-♀ had C for one site; *Mmd*-♂ had C and T for two sites; *Mmm*-♂ had C and T for two sites; *Mmm* x *Mmd*-♂ had C and T for one site; *Mmd* x *Mmm*-♀ had C and T for three sites; *Mmd* x *Mmm*-♂ had C and T for 4 sites; and *Mmm*-♀ had C and T for two sites and C for one site (Table 9 and Table 10).

Discussion

I examined the methylation patterns of five genes within the *M. m. musculus* and *M. m. domesticus* subspecies and their hybrids. The genes I examined were *Mcts2*, *Nap1l5*, *Peg10*, *Zac1*, and *Zim2*. I amplified the DMD region of each of these genes, and then I cloned and sequenced the regions. I compared the results obtained within the hybrids to that observed within the parental samples. I expected each sample to yield one methylated and one unmethylated allele for each gene. I also expected there to be some CG sites that were methylated on both alleles. I observed decreases and increases of

methylation within the hybrids and parents. There were changes in methylation within the hybrids for each gene except *Mcts2, Peg10,* and *Zim2*. There was disruption in methylation within the parental samples for each gene except *Zac1*. The hybrid sample *Mmm* x *Mmd*-♀ showed disruption in methylation within two genes while the parental organisms had similar methylation levels. The *Mmd* x *Mmm*-♂ and *Mmm* x *Mmd*-♂ hybrid samples did not yield disruption in methylation within any of the genes.

Those samples that yielded changes in methylation possibly have had disruption in expression. DNA methylation can cause changes in the structure of the DNA molecule, which can prevent gene expression (Das and Singal, 2004; Jones and Takai, 2001). An increase in methylation could possibly result in a decrease in the gene expression level. A decrease in methylation, however, could possibly result in an increase in the gene expression level. The decrease in methylation will not necessarily cause biallelic expression (Jones and Takai, 2001; Tycko and Morison, 2002; Rainier et al., 1993). The hybrid and parental samples showed both increases and decreases in methylation, which suggests that those samples had increases and decreases in expression within each corresponding gene.

Previous studies have shown that disruptions in methylation patterns are present in mouse hybrids within the *Mus* genus. In *M. musculus – M. caroli* hybrids, researchers have discovered a loss of methylation in retroelements (Brown et al., 2008, 2012). The promoters of the *Oct4* and *Nanog* genes were found to be demethylated in *M. musculus – M. caroli* hybrids (Battulin et al., 2009). Loss of methylation is observed within patients with diabetes mellitus and hypermethylation is associated with cancers (Arima et al., 2006).

DNA methylation has been found to vary among individuals. This individual variation was observed in a study which examined Wilms' tumors within humans, in which two imprinted genes, *Igf2* and *H19*, showed a change in expression in only a portion of the individuals studied (Rainier et al., 1993). Individual variation was also observed within a study using *Mus musculus* and *Mus spretus* hybrids, in which only a percentage of the samples examined yielded a disruption in the expression of the *Peg1* imprinted gene (Shi et al., 2004, 2005). Therefore, the disruptions in methylation observed within this experiment may be due to individual variation.

Reproductive isolation can be created as genetic differences accumulate. Such reproductive isolation is required for speciation to occur (Good et al., 2008a, 2008b; Palumbi, 1994; Turner et al., 2012). Genetic differences between populations can be created through a number of events or occasions. The linkage between genetic variation and reproductive isolation is not fully understood within the separate subspecies *M. m. musculus* and *M. m. domesticus*. However, genetic differences leading to reproductive isolation have been observed within genes, such as the *Prdm9* locus, involved in gamete production, development, and mate recognition (Bhattacharyya et al., 2013; Flachs et al., 2012, 2014; Geraldes et al., 2011; Mihola et al., 2009; Palumbi, 1994). The genes that showed disruption within the mouse hybrids of this experiment were *Nap1l5* and *Zac1*, which are associated with development and several diseases. The *Mcts2*, *Nap1l5*, *Peg10*, and *Zim2* genes also yielded differences in methylation between the two parental subspecies. The *Mcts2*, *Peg10*, and *Zim2* genes are also important in growth and development. In total, the parents showed five increases and three decreases in methylation, while the hybrids yielded one increase and four decreases. All of this data

suggests that each of these genes showed differences between the methylation patterns of the parental and/or hybrid samples. Because each of the genes have similar functions, there is not a clear association between gene functions and methylation patterns.

The *Zim2* gene showed an increase in methylation in one parental sample and does not have a fully understood function. The *Zim2* gene is the only maternally expressed gene examined. Among mammals, conservation in methylation has been observed within paternally expressed imprinted genes; however, there is a lack of conservation within maternally expressed genes (Hutter et al., 2010b, 2010c). There does not seem to be an association between the genomic imprinting pattern of the gene and the methylation pattern observed in this experiment. Both maternally and paternally expressed imprinted genes yielded disruption in methylation within the hybrids and parental species. I believe more maternally expressed genes should be examined to identify if there is a link with the conservation observed. Within the hybrids and parents, there does also appear to be differences in methylation between the males and females. More methylation changes appear to occur within females versus males, which possibly suggests that there is variation between individuals. I feel that more parental and hybrid samples and clones should be examined to ensure that both alleles were sequenced and to determine if individual variation had been observed.

Table 2. *Mcts2* Methylation Analysis of each Sample after Cloning. Sequence notes for a 310 bp segment of the DMD region of the *Mcts2* gene. This region was amplified within bisulfite-modified DNA and then cloned using a TOPO TA cloning vector. Two (M-m, MxD-m, and DxM-f), three (M-f), four (MxD-f), or five (D-f, D-m, and DxM-m) clones were chosen for each sample, and the region inserted into the vector was amplified. The samples were then sequenced through GeneWiz in the forward and reverse directions. The sequences were examined through the program Geneious 7 and 33 differential CG and non-CG sites were identified and compared across the samples. The base pair location of each site is listed along with the bases appearing at these sites for all available clones for each sample. The two columns within each sample column represent the two alleles determined by the sequences obtained. Blue cells represent CG sites where both alleles showed TG. The last row represents the percentage of CG sites that yielded a decrease (-) in methylation.

MCTS2 Gene																	
Site #	**Base Pairs of Sequence**	**D - f**		**D - m**		**M - f**		**M - m**		**D x M - f**		**D x M - m**		**M x D - f**		**M x D - m**	
1	7 and 8	CG	TG	CG	TG	CG	TG	CG	TG	CG	TG	TG	TG	CG	TG	TG	TG
2	10 and 11	CG	TG	CG	TG	CG	TG	CG	TG	TG	TG	TG	TG	CG	TG	TG	TG
3	41 and 42	CG	TG	CG	TG	CG	TG	TG	TG	TG	TG	TG	TG	CG	TG	TG	TG
4	51 and 52	CG	TG	CG	TG	CG	TG	TG	TG	TG	TG	TG	TG	CG	TG	TG	TG
5	70 and 71	CG	TG	CG	TG	CG	TG	TG	TG	TG	TG	TG	TG	CG	TG	TG	TG
6	72 and 73	CG	TG	CG	TG	CG	TG	TG	TG	TG	TG	TG	TG	CG	TG	TG	TG
7	79 and 80	CG	TG	CG	TG	CG	TG	TG	TG	TG	TG	TG	TG	CG	TG	TG	TG
8	81 and 82	CG	TG	CG	TG	CG	TG	TG	TG	TG	TG	TG	TG	CG	TG	TG	TG
9	86 and 87	CG	TG	CG	TG	CG	TG	TG	TG	TG	TG	TG	TG	CG	TG	TG	TG
10	88 and 89	CG	TG	CG	TG	CG	TG	TG	TG	TG	TG	TG	TG	CG	TG	TG	TG
11	90 and 91	CG	TG	CG	TG	CG	TG	TG	TG	TG	TG	TG	TG	CG	TG	TG	TG
12	101 and 102	CG	TG	CG	TG	CG	TG	TG	TG	TG	TG	TG	TG	CG	TG	TG	TG
13	111 and 112	TG	TG	CG	TG	CG	TG	TG	TG	TG	TG	TG	TG	CG	TG	TG	TG
14	124 and 125	CG	TG	CG	TG	CG	TG	TG	TG	TG	TG	TG	TG	CG	TG	TG	TG
15	128 and 129	CG	TG	CG	TG	CG	TG	TG	TG	TG	TG	TG	TG	CG	TG	TG	TG
16	130 and 131	CG	TG	CG	TG	CG	TG	TG	TG	TG	TG	TG	TG	CG	TG	TG	TG
17	155 and 156	CG	TG	CG	TG	CG	TG	TG	TG	TG	CG	TG	TG	CG	TG	TG	TG
18	167 and 168	CG	TG	CG	TG	CG	TG	TG	TG	TG	CG	TG	TG	CG	TG	TG	TG
19	176 and 177	CG	TG	CG	TG	CG	TG	TG	TG	TG	TG	TG	TG	CG	TG	TG	TG
20	181 and 182	CG	TG	CG	TG	CG	TG	TG	TG	TG	TG	TG	TG	CG	TG	TG	TG
21	204 and 205	CG	TG	CG	TG	CG	TG	TG	TG	TG	TG	TG	TG	CG	TG	TG	TG
22	212 and 213	TG	TG	TG	TG	CG	TG	TG	TG	TG	TG	TG	TG	CG	TG	TG	TG
23	223 and 224	CG	TG	CG	TG	CG	TG	TG	TG	TG	TG	TG	TG	NA	TG	TG	TG
24	230 and 231	CG	TG	CG	TG	CG	TG	TG	TG	TG	TG	TG	TG	NA	TG	TG	TG
25	242 and 243	CG	TG	CG	TG	NA	NA	NA	NA	NA	NA	NA	NA	CG	TG	TG	TG
26	249 and 250	CG	TG	CG	TG	NA	NA	NA	NA	NA	NA	NA	NA	CG	TG	TG	TG
27	275 and 276	CG	TG	CG	TG	CG	TG	TG	TG	TG	TG	TG	TG	CG	TG	TG	TG
28	287 and 288	CG	TG	CG	TG	CG	TG	TG	TG	TG	TG	TG	TG	CG	TG	CG	TG
29	293 and 294	CG	TG	CG	TG	CG	TG	TG	TG	TG	TG	TG	TG	CG	TG	CG	TG
30	295 and 296	TG	TG	TG	TG	TG	TG	TG	TG	CG	TG	TG	TG	TG	TG	TG	TG
31	190	T	T	T	C	T	T	T	T	T	T	T	T	T	T	T	T
32	210	T	T	T	T	C	T	T	T	T	T	T	T	T	T	T	T
33	310	C	T	T	C	C	T	T	T	T	T	T	T	C	T	C	T
	Percent of Change	-10.00%		-6.70%		-3.30%		-86.70%		-80.00%		-93.30%		-3.30%		-93.30%	

Table 3. *Mcts2* Methylation Analysis of Samples M-m, DxM-f, DxM-m, and MxD-m after Bisulfite-Modification. Sequence notes for a 310 bp segment of the DMD region of the *Mcts2* gene. This region was amplified within bisulfite-modified DNA. The samples were then sequenced through GeneWiz in the forward and reverse directions. The sequences were examined through the program Geneious 7 and 33 differential CG and non-CG sites were identified and compared across the samples. The base pair location of each site is listed along with the bases appearing at these sites.

MCTS2 Gene					
Site #	Base Pairs of Sequence	Bi-M-m	Bi-D x M - f	Bi-D x M - m	Bi-M x D - m
1	7 and 8	NA	NA	NA	NA
2	10 and 11	NA	NA	NA	NA
3	41 and 42	CG,TG	CG,TG	CG,TG	CG,TG
4	51 and 52	CG,TG	CG,TG	CG,TG	CG,TG
5	70 and 71	CG,TG	CG,TG	CG,TG	CG,TG
6	72 and 73	CG,TG	CG,TG	CG,TG	CG,TG
7	79 and 80	CG,TG	CG,TG	CG,TG	CG,TG
8	81 and 82	CG,TG	CG,TG	CG,TG	CG,TG
9	86 and 87	CG,TG	CG,TG	CG,TG	CG,TG
10	88 and 89	CG,TG	CG,TG	CG,TG	CG,TG
11	90 and 91	CG,TG	CG,TG	CG,TG	CG,TG
12	101 and 102	CG,TG	CG,TG	CG,TG	CG,TG
13	111 and 112	CG,TG	CG,TG	CG,TG	CG,TG
14	124 and 125	CG,TG	CG,TG	CG,TG	CG,TG
15	128 and 129	CG,TG	CG,TG	CG,TG	CG,TG
16	130 and 131	CG,TG	CG,TG	CG,TG	CG,TG
17	155 and 156	CG,TG	CG,TG	CG,TG	CG,TG
18	167 and 168	CG,TG	CG,TG	CG,TG	CG,TG
19	176 and 177	CG,TG	CG,TG	CG,TG	CG,TG
20	181 and 182	CG,TG	CG,TG	CG,TG	CG,TG
21	204 and 205	CG,TG	CG,TG	CG,TG	CG,TG
22	212 and 213	CG,TG	CG,TG	CG,TG	CG,TG
23	223 and 224	CG,TG	CG,TG	CG,TG	CG,TG
24	230 and 231	CG,TG	CG,TG	CG,TG	CG,TG
25	242 and 243	NA	NA	NA	NA
26	249 and 250	NA	NA	CG,TG	NA
27	275 and 276	CG,TG	CG,TG	NA	NA
28	287 and 288	NA	NA	NA	NA
29	293 and 294	NA	NA	NA	NA
30	295 and 296	NA	NA	NA	NA
31	190	T	T	T	T
32	210	C,T	C,T	C,T	T
33	310	C	C	C	C

Table 4. *Nap1l5* Methylation Analysis of each Sample after Cloning. Sequence notes for a 234 bp segment of the DMD region of the *Nap1l5* gene. This region was amplified within bisulfite-modified DNA and then cloned using a TOPO TA cloning vector. Five clones were chosen for each sample, and the region inserted into the vector was amplified. The samples were then sequenced through GeneWiz in the forward and reverse directions. The sequences were examined through the program Geneious 7 and 26 differential CG and non-CG sites were identified and compared across the samples. The base pair location of each site is listed along with the bases appearing at these sites for all available clones for each sample. The two columns within each sample column represent the two alleles determined by the sequences obtained. Blue cells represent CG sites where both alleles showed TG while orange cells represent CG sites where both alleles showed CG. The last row represents the percentage of CG sites that yielded an increase (+) or decrease (-) in methylation.

NAP1L5 Gene																
Site #	Base Pairs of Sequence	D - f		D - m		M - f		M - m		D x M - f		D x M - m		M x D - f		M x D - m	
1	18 and 19	CG	TG	CG	TG	CG	TG	CG	CG	CG	TG	CG	TG	CG	CG	CG	CG
2	20 and 21	CG	TG	CG	TG	CG	CG	CG	TG	TG	TG	CG	TG	CG	CG	CG	CG
3	27 and 28	CG	TG	CG	TG	CG	TG	CG	TG	CG	TG	CG	TG	CG	TG	CG	CG
4	29 and 30	CG	TG	CG	TG	CG	TG	CG	TG	TG	TG	CG	TG	CG	TG	CG	CG
5	47 and 48	CG	TG	CG	TG	CG	TG	CG	CG	CG	TG	CG	TG	CG	TG	CG	CG
6	51 and 52	CG	TG	CG	TG	CG	CG	CG	TG	CG	TG	CG	TG	CG	TG	CG	TG
7	53 and 54	CG	TG	CG	TG	CG	TG	CG	TG	CG	TG	CG	TG	CG	TG	CG	TG
8	62 and 63	CG	TG	CG	TG	CG	TG	CG	TG	CG	TG	CG	TG	CG	TG	CG	CG
9	74 and 75	CG	TG	CG	TG	CG	TG	CG	TG	CG	TG	CG	TG	CG	CG	CG	CG
10	78 and 79	TG	CG	CG	TG	CG	TG	CG	TG	CG	TG	CG	TG	CG	TG	CG	TG
11	80 and 81	CG	TG	CG	TG	CG	CG	CG	TG	CG	TG	CG	TG	CG	TG	CG	CG
12	89 and 90	TG	CG	CG	CG	CG	CG	CG	CG	CG	TG	CG	TG	CG	CG	CG	CG
13	101 and 102	CG	TG	CG	TG	CG	CG	CG	CG	CG	TG	CG	TG	CG	TG	CG	CG
14	116 and 117	TG	CG	CG	TG	CG	TG	CG	CG	CG	TG	CG	TG	CG	CG	CG	CG
15	122 and 123	TG	CG	CG	TG	CG	TG	CG	TG	CG	TG	CG	TG	CG	TG	CG	TG
16	127 and 128	TG	CG	CG	TG	CG	TG	CG	CG	CG	TG	CG	TG	CG	CG	CG	CG
17	137 and 138	TG	CG	CG	TG	CG	TG	CG	TG	CG	TG	CG	TG	CG	TG	CG	CG
18	152 and 153	CG	TG	CG	TG	CG	CG	CG	CG	CG	TG	CG	TG	CG	CG	CG	TG
19	158 and 159	CG	TG	CG	TG	CG	CG	CG	TG	CG	TG	CG	TG	CG	CG	CG	TG
20	175 and 176	CG	TG	CG	TG	CG	CG	CG	CG	CG	TG	CG	TG	CG	CG	CG	TG
21	197 and 198	CG	TG	CG	TG	CG	TG	CG	TG	CG	TG	CG	TG	CG	CG	CG	TG
22	216 and 217	CG	TG	CG	TG	CG	CG	CG	CG	CG	TG	CG	TG	CG	CG	CG	CG
23	24	T	C	T	T	T	T	T	T	T	T	T	T	T	T	T	T
24	42	T	T	T	T	T	T	T	T	T	T	T	T	T	T	T	C
25	71	T	T	T	T	T	T	T	T	T	T	C	T	T	T	T	C
26	196	T	T	T	T	C	T	T	T	T	T	T	T	T	T	T	T
	Percent of Change	0%		4.50%		40.90%		40.90%		-9.10%		0%		50%		63.60%	

Table 5. *Nap1l5* Methylation Analysis of Samples D-f and MxD-m after Bisulfite-Modification. Sequence notes for a 234 bp segment of the DMD region of the *Nap1l5* gene. This region was amplified within bisulfite-modified DNA. The samples were then sequenced through GeneWiz in the forward and reverse directions. The sequences were examined through the program Geneious 7 and 26 differential CG and non-CG sites were identified and compared across the samples. The base pair location of each site is listed along with the bases appearing at these sites.

NAP1L5 Gene			
Site #	**Base Pairs of Sequence**	**Bi-D - f**	**Bi-M x D - m**
1	18 and 19	NA	NA
2	20 and 21	CG,TG	CG,TG
3	27 and 28	CG,TG	CG,TG
4	29 and 30	CG,TG	CG,TG
5	47 and 48	CG,TG	CG,TG
6	51 and 52	CG,TG	CG,TG
7	53 and 54	CG,TG	CG,TG
8	62 and 63	CG,TG	CG,TG
9	74 and 75	CG,TG	CG,TG
10	78 and 79	CG,TG	CG,TG
11	80 and 81	CG,TG	CG,TG
12	89 and 90	CG,TG	CG,TG
13	101 and 102	CG,TG	CG,TG
14	116 and 117	CG,TG	CG,TG
15	122 and 123	CG,TG	CG,TG
16	127 and 128	CG,TG	CG,TG
17	137 and 138	CG,TG	CG,TG
18	152 and 153	CG,TG	CG,TG
19	158 and 159	CG,TG	CG,TG
20	175 and 176	CG,TG	CG,TG
21	197 and 198	CG,TG	CG,TG
22	216 and 217	CG,TG	CG,TG
23	24	T	T
24	42	T	T
25	71	T	T
26	196	C,T	C,T

Table 6. *Peg10* Methylation Analysis of each Sample after Cloning. Sequence notes for a 228 bp segment of the DMD region of the *Peg10* gene. This region was amplified within bisulfite-modified DNA and then cloned using a TOPO TA cloning vector. Three (M-f), four (DxM-m), or five (D-f, D-m, M-m, MxD-f, MxD-m, and DxM-f) clones were chosen for each sample, and the region inserted into the vector was amplified. The samples were then sequenced through GeneWiz in the forward and reverse directions. The sequences were examined through the program Geneious 7 and 30 differential CG and non-CG sites were identified and compared across the samples. The base pair location of each site is listed along with the bases appearing at these sites for all available clones for each sample. The two columns within each sample column represent the two alleles determined by the sequences obtained. Orange cells represent CG cites where both alleles showed CG. The last row represents the percentage of CG sites that yielded an increase (+) in methylation.

PEG10 Gene																	
Site #	Base Pairs of Sequence	D - f		D - m		M - f		M - m		D x M - f		D x M - m		M x D - f		M x D - m	
1	10 and 11	CG	TG	CG	TG	CG	CG	CG	TG	CG	TG	CG	TG	CG	TG	CG	TG
2	18 and 19	CG	TG	CG	TG	CG	CG	CG	TG	CG	TG	CG	TG	CG	TG	CG	TG
3	25 and 26	CG	TG	CG	TG	CG	CG	CG	TG	CG	TG	CG	TG	CG	TG	CG	TG
4	27 and 28	CG	TG	CG	TG	CG	CG	CG	TG	CG	TG	CG	TG	CG	TG	CG	TG
5	53 and 54	CG	TG	CG	TG	CG	CG	CG	TG	CG	TG	CG	TG	CG	TG	CG	TG
6	73 and 74	CG	TG	CG	TG	CG	CG	CG	TG	CG	TG	CG	TG	CG	TG	CG	TG
7	95 and 96	CG	TG	CG	TG	CG	CG	CG	TG	CG	TG	CG	TG	CG	TG	CG	TG
8	108 and 109	CG	TG	CG	TG	CG	CG	CG	TG	CG	TG	CG	TG	CG	TG	CG	TG
9	115 and 116	CG	TG	CG	TG	CG	CG	CG	TG	CG	TG	CG	TG	CG	TG	CG	TG
10	130 and 131	CG	TG	CG	TG	CG	CG	CG	TG	CG	TG	CG	TG	CG	TG	CG	TG
11	132 and 133	CG	TG	CG	TG	CG	CG	CG	TG	CG	TG	CG	TG	CG	TG	CG	TG
12	139 and 140	CG	TG	CG	TG	CG	CG	CG	TG	CG	TG	CG	TG	CG	TG	CG	TG
13	144 and 145	CG	TG	CG	TG	CG	CG	CG	TG	CG	TG	CG	TG	CG	TG	CG	TG
14	156 and 157	CG	TG	CG	TG	CG	CG	CG	TG	CG	TG	CG	TG	CG	TG	CG	TG
15	161 and 162	CG	TG	CG	TG	CG	CG	CG	TG	CG	TG	CG	TG	CG	TG	CG	TG
16	163 and 164	CG	TG	CG	TG	CG	TG	CG	TG	CG	TG	CG	TG	CG	TG	CG	TG
17	179 and 180	CG	TG	CG	TG	CG	CG	CG	TG	CG	TG	CG	TG	CG	TG	CG	TG
18	184 and 185	CG	TG	CG	TG	CG	CG	CG	TG	CG	TG	CG	TG	CG	TG	CG	TG
19	187 and 188	CG	TG	CG	TG	CG	CG	CG	TG	CG	TG	CG	TG	CG	TG	CG	TG
20	189 and 190	CG	TG	CG	TG	CG	CG	CG	TG	CG	TG	CG	TG	CG	TG	CG	TG
21	206 and 207	CG	TG	CG	TG	CG	CG	CG	TG	CG	TG	CG	TG	CG	TG	CG	TG
22	214 and 215	CG	TG	CG	TG	CG	CG	CG	TG	CG	TG	CG	TG	CG	TG	CG	TG
23	143	C	T	C	T	C	T	C	T	C	T	C	T	C	T	C	T
24	155	T	C	C	T	C	T	T	T	C	T	C	T	C	T	C	T
25	160	C	T	C	T	C	T	C	T	C	T	C	T	C	T	C	T
26	203	T	T	T	T	T	T	T	T	T	T	T	T	T	C	T	T
27	211	T	T	T	T	T	C	T	T	T	T	T	T	T	T	T	T
28	213	T	T	T	T	T	T	T	T	C	T	T	T	T	T	T	T
29	216	T	T	T	T	T	T	T	T	T	T	T	T	C	T	T	T
30	228	C	T	C	T	C	C	C	T	C	T	C	T	C	T	C	T
	Percent of Change	0%		0%		95.50%		0%		0%		0%		0%		0%	

Table 7. *Zac1* Methylation Analysis of each Sample after Cloning. Sequence notes for a 254 bp segment of the DMD region of the *Zac1* gene. This region was amplified within bisulfite-modified DNA and then cloned using a TOPO TA cloning vector. Two (D-f), three (MxD-f), four (M-f, MxD-m, DxM-f), or five (D-m, M-m, and DxM-m) clones were chosen for each sample, and the region inserted into the vector was amplified. The samples were then sequenced through GeneWiz in the forward and reverse directions. The sequences were examined through the program Geneious 7 and 18 differential CG and non-CG sites were identified and compared across the samples. The base pair location of each site is listed along with the bases appearing at these sites for all available clones for each sample. The two columns within each sample column represent the two alleles determined by the sequences obtained. Blue cells represent CG sites where both alleles showed TG. The last row represents the percentage of CG sites that yielded a decrease (-) in methylation.

ZAC1 Gene																	
Site #	Base Pairs of Sequence	D - f		D - m		M - f		M - m		D x M - f		D x M - m		M x D - f		M x D - m	
1	11 and 12	TG	TG	CG	TG	CG	TG	CG	TG	CG	TG	CG	TG	TG	TG	CG	TG
2	16 and 17	TG	TG	CG	TG	CG	TG	CG	TG	TG	TG	CG	TG	TG	TG	CG	TG
3	33 and 34	TG	TG	CG	TG	CG	TG	CG	TG	CG	TG	CG	TG	TG	TG	CG	TG
4	38 and 39	TG	TG	CG	TG	CG	TG	CG	TG	CG	TG	CG	TG	TG	TG	CG	TG
5	40 and 41	TG	TG	CG	TG	CG	TG	CG	TG	CG	TG	CG	TG	TG	TG	CG	TG
6	54 and 55	TG	TG	CG	TG	CG	TG	CG	TG	CG	TG	CG	TG	TG	TG	CG	TG
7	65 and 66	TG	TG	CG	TG	CG	TG	CG	TG	CG	TG	CG	TG	TG	TG	CG	TG
8	76 and 77	TG	TG	CG	TG	CG	TG	CG	TG	CG	TG	CG	TG	TG	CG	CG	TG
9	90 and 91	TG	TG	CG	TG	CG	TG	CG	TG	CG	TG	CG	TG	CG	TG	CG	TG
10	107 and 108	TG	TG	CG	TG	CG	TG	CG	TG	CG	TG	CG	TG	CG	TG	CG	TG
11	121 and 122	TG	TG	CG	TG	CG	TG	CG	TG	CG	TG	CG	TG	CG	TG	CG	TG
12	140 and 141	TG	TG	CG	TG	CG	TG	CG	TG	TG	TG	CG	TG	CG	TG	CG	TG
13	184 and 185	TG	TG	CG	TG	CG	TG	CG	TG	CG	TG	CG	TG	CG	TG	CG	TG
14	207 and 208	TG	TG	CG	TG	CG	TG	CG	TG	CG	TG	CG	TG	CG	TG	CG	TG
15	213 and 214	TG	TG	CG	TG	CG	TG	CG	TG	CG	TG	CG	TG	CG	TG	CG	TG
16	71	T	T	T	T	T	T	T	T	C	T	T	T	T	T	T	T
17	79	T	T	T	T	T	T	T	T	T	T	T	T	T	T	C	T
18	249	T	T	C	T	T	T	T	T	T	T	T	T	T	T	T	T
	Percent of Change	-100%		0%		0%		0%		-13.30%		0%		-46.70%		0%	

Table 8. *Zac1* Methylation Analysis of Sample D-f after Bisulfite-Modification. Sequence notes for a 254 bp segment of the DMD region of the *Zac1* gene. This region was amplified within bisulfite-modified DNA. The samples were then sequenced through GeneWiz in the forward and reverse directions. The sequences were examined through the program Geneious 7 and 18 differential CG and non-CG sites were identified and compared across the samples. The base pair location of each site is listed along with the bases appearing at these sites.

ZAC1 Gene		
Site #	**Base Pairs of Sequence**	**Bi-D - f**
1	11 and 12	NA
2	16 and 17	CG,TG
3	33 and 34	CG,TG
4	38 and 39	CG,TG
5	40 and 41	CG,TG
6	54 and 55	CG,TG
7	65 and 66	CG,TG
8	76 and 77	CG,TG
9	90 and 91	CG,TG
10	107 and 108	CG,TG
11	121 and 122	CG,TG
12	140 and 141	CG,TG
13	184 and 185	CG,TG
14	207 and 208	CG,TG
15	213 and 214	CG,TG
16	71	T
17	79	T
18	249	T

Table 9. *Zim2* Methylation Analysis of each Sample after Cloning. Sequence notes for a 278 bp segment of the DMD region of the *Zim2* gene. This region was amplified within bisulfite-modified DNA and then cloned using a TOPO TA cloning vector. Two (D-f, DxM-m, and MxD-m), three (M-f), four (M-m), five (MxD-f and D-m), or seven (DxM-f) clones were chosen for each sample, and the region inserted into the vector was amplified. The samples were then sequenced through GeneWiz in the forward and reverse directions. The sequences were examined through the program Geneious 7 and 28 differential CG and non-CG sites were identified and compared across the samples. The base pair location of each site is listed along with the bases appearing at these sites for all available clones for each sample. The two columns within each sample column represent the two alleles determined by the sequences obtained. Orange cells represent CG sites where both alleles showed CG. The last row represents the percentage of CG sites that yielded an increase (+) in methylation.

ZIM2 Gene																	
Site #	Base Pairs of Sequence	D - f		D - m		M - f		M - m		D x M - f		D x M - m		M x D - f		M x D - m	
1	2 and 3	CG	TG	CG	TG	CG	CG	CG	TG	CG	TG	CG	TG	CG	TG	CG	TG
2	17 and 18	CG	TG	CG	TG	CG	CG	CG	TG	CG	TG	CG	TG	CG	TG	CG	TG
3	28 and 29	CG	TG	CG	TG	CG	CG	CG	TG	CG	TG	CG	TG	CG	TG	CG	TG
4	30 and 31	CG	TG	CG	TG	CG	CG	CG	TG	CG	TG	CG	TG	CG	TG	CG	TG
5	36 and 37	CG	TG	CG	TG	CG	CG	CG	TG	CG	TG	CG	TG	CG	TG	CG	TG
6	67 and 68	CG	TG	CG	TG	CG	CG	CG	TG	CG	TG	CG	TG	CG	TG	CG	TG
7	108 and 109	CG	TG	CG	TG	CG	TG	CG	TG	CG	TG	CG	TG	CG	TG	CG	TG
8	124 and 125	CG	TG	CG	TG	CG	CG	CG	TG	CG	TG	CG	TG	CG	TG	CG	TG
9	141 and 142	CG	TG	CG	TG	CG	CG	CG	TG	CG	TG	CG	TG	CG	TG	CG	TG
10	152 and 153	CG	TG	CG	TG	CG	CG	CG	TG	CG	TG	CG	TG	CG	TG	CG	TG
11	162 and 163	CG	TG	CG	TG	CG	CG	CG	TG	CG	TG	CG	TG	CG	TG	CG	TG
12	189 and 190	CG	CG	CG	TG	CG	CG	CG	TG	CG	TG	CG	TG	CG	TG	CG	TG
13	193 and 194	CG	CG	CG	TG	CG	CG	CG	TG	CG	TG	CG	TG	CG	TG	CG	TG
14	197 and 198	CG	CG	CG	TG	CG	CG	CG	TG	CG	TG	CG	TG	CG	TG	CG	TG
15	200 and 201	CG	CG	CG	TG	CG	CG	CG	TG	CG	TG	CG	TG	CG	TG	CG	TG
16	203 and 204	CG	CG	CG	TG	CG	CG	CG	TG	CG	TG	CG	TG	CG	TG	CG	TG
17	231 and 232	CG	CG	CG	TG	CG	CG	CG	TG	CG	TG	CG	TG	CG	TG	CG	NA
18	243 and 244	CG	CG	CG	TG	CG	CG	CG	TG	CG	NA	CG	NA	CG	TG	CG	TG
19	250 and 251	CG	CG	CG	TG	CG	TG	CG	TG	CG	TG	CG	TG	CG	TG	CG	TG
20	258 and 259	CG	CG	CG	TG	CG	CG	CG	TG	CG	TG	CG	TG	CG	TG	CG	TG
21	260 and 261	CG	CG	CG	TG	CG	CG	CG	TG	CG	TG	CG	TG	CG	TG	CG	TG
22	27	T	T	T	C	T	T	T	T	T	T	T	T	T	T	T	T
23	63	T	T	T	T	T	T	T	T	C	T	T	T	C	T	T	T
24	91	T	T	T	T	T	T	T	T	T	T	C	T	T	T	T	T
25	183	T	T	T	T	T	T	T	T	T	T	T	T	T	C	T	T
26	241	T	T	T	T	T	T	C	T	T	T	T	T	T	T	T	T
27	275	T	T	T	T	T	T	T	T	T	T	T	T	T	C	T	T
28	278	C	C	C	T	C	C	C	T	C	T	C	T	C	C	C	T
	Percent of Change	47.60%		0%		90.50%		0%		0%		0%		0%		0%	

Table 10. *Zim2* Methylation Analysis of Samples M-f, DxM-f, and DxM-m after Bisulfite-Modification. Sequence notes for a 278 bp segment of the DMD region of the *Zim2* gene. This region was amplified within bisulfite-modified DNA. The samples were then sequenced through GeneWiz in the forward and reverse directions. The sequences were examined through the program Geneious 7 and 28 differential CG and non-CG sites were identified and compared across the samples. The base pair location of each site is listed along with the bases appearing at these sites.

ZIM2 Gene				
Site #	**Base Pairs of Sequence**	**Bi-M - f**	**Bi-D x M - f**	**Bi-D x M - m**
1	2 and 3	NA	NA	NA
2	17 and 18	CG,TG	CG,TG	CG,TG
3	28 and 29	CG,TG	CG,TG	CG,TG
4	30 and 31	CG,TG	CG,TG	CG,TG
5	36 and 37	CG,TG	CG,TG	NA
6	67 and 68	CG,TG	CG,TG	CG,TG
7	108 and 109	CG,TG	CG,TG	CG,TG
8	124 and 125	CG,TG	CG,TG	CG,TG
9	141 and 142	CG,TG	CG,TG	CG,TG
10	152 and 153	CG,TG	CG,TG	CG,TG
11	162 and 163	CG,TG	CG,TG	CG,TG
12	189 and 190	CG,TG	CG,TG	CG,TG
13	193 and 194	CG,TG	CG,TG	CG,TG
14	197 and 198	CG,TG	CG,TG	CG,TG
15	200 and 201	CG,TG	CG,TG	CG,TG
16	203 and 204	CG,TG	CG,TG	CG,TG
17	231 and 232	NA	NA	NA
18	243 and 244	NA	NA	NA
19	250 and 251	NA	NA	NA
20	258 and 259	NA	NA	NA
21	260 and 261	NA	NA	NA
22	27	T	T	T
23	63	C,T	C,T	C,T
24	91	T	T	T
25	183	T	T	T
26	241	C,T	C,T	C,T
27	275	T	T	T
28	278	C	C	C

Table 11. Summary of Methylation Analyses. Summary of the results for each gene examined within *Mus musculus musculus* (Mus) and *Mus musculus domesticus* (Dom) and their hybrids. Males (m) and females (f) were examined. A region of each gene was amplified within bisulfite-modified DNA. The samples were cloned and then sequenced through Genewiz in the forward and reverse directions. The sequences were examined through the program Geneious 7, and differential CG sites were identified and compared across the samples. The circles indicate a decrease in methylation; the squares indicate an increase in methylation; and the checkmarks indicate that methylation is maintained.

	Dom-f	Dom-m	Mus-f	Mus-m	Dom x Mus-f	Dom x Mus-m	Mus x Dom-f	Mus x Dom-m
Mcts2	○	○	○	✓	✓	✓	○	✓
Nap1l5	✓	■	■	■	○	✓	■	✓
Peg10	✓	✓	■	✓	✓	✓	✓	✓
Zac1	✓	✓	✓	✓	○	✓	○	✓
Zim2	■	✓	✓	✓	✓	✓	✓	✓

Table 12. Primers used in PCR to Amplify Bisulfite-Modified DNA and *E. coli* Vectors. A description of the primers used in PCR. The name of the primers, the name of the gene associated with the primers, and the primer sequences are listed here. The primer sequences were obtained from WAMIDEX or the TOPO TA Cloning Kit (Invitrogen) (Schulz et al., 2008). The symbol "Bi" indicates that the particular primer was associated with bisulfite-modified template and amplified the DMD associated with the gene.

Gene	Primer Name	Primer Sequence	Annealing Temperature
Mcts2	Mcts2-Bi-3-F	GGATTTTYGGGGATGTTTGGGATAG	51^{o}C
	Mcts2-Bi-3-R	ACTTTACRACTATATAAAATCCAATAACTTCC	
Nap1l5	Nap1l5-Bi-3-F	AYGGAATTGGGTAAGTTTTTTATAAAG	46^{o}C
	Nap1l5-Bi-3-R	CACAACTACAAAACCTCTCTAAACC	
Zim2	Zim2-Bi-4-F	YGTAGTTTGTAGTTTTGTTAGTTATTTTTGGGAG	52^{o}C
	Zim2-Bi-4-R	AAATATCCCRCAACCCTTACTACAAAC	
Peg10	Peg10-Bi-2-F	TTGGYGTTTTTTTTTTTAGGATTTTTTTATATAAGG	48^{o}C
	Peg10-Bi-2-R	AAAAAATCCTAACCATACTCACCACAC	
Zac1	Zac1-Bi-3-F	AATTTGGGTGTTTTAGTTGTAGTTAGAGATGTAG	52^{o}C
	Zac1-Bi-3-R	ATTACRCTCTAAATTCTCCCAAAAATTC	
Cloning Vector	M13F	GTAAAACGACGGCCAGTGAATTGTAATACGACTCACTATAGGGCGAATTGAATTTAGCGGCCGCGAATTCGCCCTT	52^{o}C
	M13R	CAGGAAACAGCTATGACCATGATTACGCCAAGCTCAGAATTAACCCTCACTAAAGGGACTAGTCCTGCAGGTTTAAACGAATTCGCCCTT	

CHAPTER THREE: EXPRESSION OF IMPRINTED GENES IN MOUSE HYBRIDS

Introduction

Genomic imprinting is a pattern of gene expression that is primarily achieved through DNA methylation at a differentially methylated domain (Reinhart et al., 2006). DNA methylation causes changes in the structure and grooves of DNA, which alters gene expression as enzymes and other cofactors cannot bind to the DNA (Jones and Takai, 2001). This change in binding causes one copy of a gene, or allele, to be silenced. Genomic silencing results in the expression of only one allele at a particular locus, and this expression pattern causes the genes to be functionally haploid (Ashbrook and Hager, 2013; Reinhart et al., 2006; Tilghman, 1999). The silencing of alleles increases the probability that individuals will develop serious conditions caused by recessive alleles (Morison et al., 2005; Virani et al., 2012). Most imprinted genes are associated with growth and pathways involved in metabolism and cell adhesion (Gregg et al., 2010).

Previous studies have shown that disruptions in genomic imprinting are present in mouse hybrids of the *Mus* genus. In *M. musculus-M. spretus* hybrids, researchers discovered a loss of imprinting in the *Mest, Peg3,* and *Snrpn* genes (Shi et al., 2004, 2005). These three genes are normally paternally expressed and are important in growth and development (Shi et al., 2004, 2005).

In this experiment, two-step qRT-PCR was performed for five imprinted genes within mouse hybrids in order to ascertain gene expression levels. The five genes I examined were *Mcts2*, *Mest*, *Nap1l5*, *H19*, and *Igf2r* (Table 1). RNA was isolated from

mouse pup tissues obtained from a lab in Eastern Michigan University. The RNA was then converted to cDNA through reverse transcriptase, which then underwent real-time PCR (Dong et al., 2013). Because RNA represents the genes that have been expressed and have undergone transcription, this process examined gene expression levels. Real-time PCR then examined the PCR amplification process in real-time (Machado et al., 2013). The reagent SYBR Green was utilized in this process. SYBR Green is a fluorescent intercalating dye that binds to newly synthesized double-stranded DNA. When the dye binds to the DNA, it fluoresces, and the fluorescence from this dye is then monitored (Dong et al., 2013; Machado et al., 2013).

Within this experiment, a value termed C_t was then analyzed, which represents the PCR cycle number in which a relative level of fluorescence was detected. The higher the C_t value, the lower the amount of RNA there is, while low C_t values represent a large amount of RNA (Dong et al., 2013; Machado et al., 2013). These C_t values were then normalized through the Pfaffl method, and the relative expression level was analyzed (Pfaffl, 2001). If the hybrid samples showed a loss of imprinting, I expected to see a higher relative expression as compared to the parental samples since the genes will yield greater expression and therefore there would be more RNA/cDNA. If the hybrid samples did not have any changes in genetic imprinting, I expected the relative expression values to be the same in the hybrids as compared to the parents. Instead, if the hybrid samples showed methylation in both alleles, I expected to see a lower relative expression since the gene will not be expressed as much from either allele as compared to the parental samples (Shi et al., 2005). Performing real-time PCR allowed me to examine the expression levels of the five imprinted genes and to determine if the DNA methylation

changes I observed for the genes *Mcts2* and *Nap1l5* affected the expression levels of those genes.

Materials and Methods

Embryo body tissues were obtained from Dr. David Kass of Eastern Michigan University. The body tissues were obtained for the samples *Mmd*-♀ (R1), *Mmd*-♂ (R2), *Mmm*-♀ (R3), *Mmm*-♂ (R4), *Mmd* x *Mmm*-♂ (R5), *Mmm* x *Mmd*-♀ (R6), and *Mmm* x *Mmd*-♂ (R7). The female parents are listed first in the hybrid notation. One male and one female of the two parental samples and an individual representing three of their four hybrids were obtained. The tissues were from 13-16 day old mouse embryos. The *Mmd* samples were of the LEWES strain, and the *Mmm* samples were of the PWK strain. RNA was isolated and extracted from these house mouse samples using the Qiagen RNAeasy® mini kit. All equipment and surfaces were wiped down with RNAase Zap. Two-step qRT-PCR was performed. First-strand cDNA was synthesized using ThermoScientific RevertAid Reverse Transciptase. Primers for qRT-PCR were obtained from the PrimerBank database and the IDT PrimeTime® database (Table 13) (PrimeTime® program, 2015; Spandidos et al., 2008, 2010; Wang and Seed, 2003). A number of primers did not successfully amplify the template (Table 16). I ran real-time PCR for six genes *H19*, *Igf2r*, *Mcts2*, *Mest*, *Nap1l5*, and *eEF-2* (Table 1). The *Eukaryotic elongation factor 2* (*eEF-2*) gene, which is a housekeeping gene, was used in order to normalize the real-time PCR data.

A primer efficiency test was done initially to ensure the primers worked properly. For each of the 6 primer sets, 4 serial dilutions (1:1, 1:10, 1:100, 1:1000 or 1:1, 1:5, 1:25, 1:125) of the template were made and then each template was run in triplicate. There

were a total of 12 reactions per primer set. RNA for the primer efficiency test was obtained from adult liver tissues of balb/c and Black57 C57/B6 mouse hybrids. These mice were obtained from Dr. Erich Ottem's lab at NMU. This template was labeled as R8. The efficiency of each primer was between 89.0% and 110%, and the R^2 value was larger than 0.900. The primer efficiency test was done with USB VeriQuest™ SYBR Green qPCR Master Mix (2X), and this reagent required an initial 2 min 50ºC incubation where any leftover RNA was broken down. The 50ºC incubation was followed by a 10 minute 95ºC incubation and a melting curve analysis. Samples were pipetted into 96-well semi-skirted plates, and the results were examined within the program BioRad iQ5.

After the primer efficiency tests, qPCR was performed. USB VeriQuest™ SYBR Green qPCR Master Mix (2X) was used in this process, and the samples were run in triplicate. There were 24 reactions per primer set where the 7 samples along with the control sample were run. For each gene or primer set, the C_t numbers of each sample were compared across the samples. The Pfaffl method was used to normalize the data, and the standard deviation of each sample's data set was calculated. The Pfaffl calculation, which produces a ratio, is $\frac{(E_{target})^{\Delta Ct\ target\ (control-treated)}}{(E_{ref})^{\Delta Ct\ ref\ (control-treated)}}$ (Pfaffl, 2001). For each gene's data set, I performed a one-way ANOVA statistical test as well as a post-Hoc Tukey HSD test in order to see if the differences observed in the expression were significant (Kramer, 1956; Tukey, 1949).

Results

I performed two-step qRT-PCR on the cDNA obtained from seven samples. I used primers to amplify a section of the coding region of the respective *H19*, *Igf2r*,

Mcts2, *Mest*, and *Nap1l5* genes. I used the Pfaffl method to normalize the C_t data. I used data for the housekeeping, *eEF-2* gene to normalize the data. The data for the *eEF-2* gene caused differences between the relative expression level scales of the genes despite any similar C_t values. I then performed a one-way ANOVA statistical test and post-Hoc Tukey HSD test on each gene's data set. I did observe that within each of the genes, there were differences in the expression levels of at least one of the hybrid samples as compared to some of the parents. Within each gene, except *Nap1l5*, at least one of the hybrid samples showed a similar expression level as compared to some of the parents. There were also differences between the expression levels of the two parental subspecies.

H19 Gene

I observed that each sample yielded decreased expression in the *H19* gene as compared to the control sample (Figure 1). The *Mmd*-♀ (R1) sample had the largest decrease in expression, and this sample had 10.57 times lower *H19* expression as compared to the control sample. This sample had significantly different expression levels as compared to the other samples ($p < 0.01$). Samples *Mmd*-♂, *Mmm*-♀, *Mmm*-♂, *Mmd* x *Mmm*-♂, and *Mmm* x *Mmd*-♀ (R2-R6) showed similar expression levels ($p > 0.05$) that were 5 to 8 times greater than that of sample *Mmd*-♀ (R1). The sample *Mmm* x *Mmd*-♂ (R7) yielded two times higher *H19* expression as compared to that of the *Mmd*-♀ (R1) sample (Figure 1). The *Mmm* x *Mmd*-♂ (R7) sample had significantly different expression levels as compared to the other samples ($p < 0.01$). Sample *Mmd*-♀ (R1) showed the greatest standard deviation of 3.54 while the sample *Mmd*-♂ (R2) yielded the lowest standard deviation of 0.44 (Figure 1). In looking at the raw C_t values observed within the *H19* qRT-PCR experiment, sample *Mmd*-♀ (R1) showed the largest average C_t

value of 34.95 (Table 14A). Samples *Mmm*-♀, *Mmm*-♂, *Mmd* x *Mmm*-♂, *Mmm* x *Mmd*-♀, and *Mmm* x *Mmd*-♂ (R3-R7) yielded similar average C_t values between 26.57 and 28.98. The control sample (R8) showed the lowest C_t value of 23.17 (Table 14A).

***Mcts2* Gene**

I observed that the samples *Mmd*-♀ (R1), *Mmd*-♂ (R2), *Mmm* x *Mmd*-♀ (R6), and *Mmm* x *Mmd*-♂ (R7) yielded increased expression in the *Mcts2* gene as compared to the control sample (Figure 2). The samples *Mmm*-♀ (R3), *Mmm*-♂ (R4), and *Mmd* x *Mmm*-♂ (R5) showed decreased expression. The *Mmd*-♂ (R2) sample yielded the largest increase in expression, and this sample had 5.0 times higher *Mcts2* expression as compared to the expression of the control sample (Figure 2). This sample had significantly different expression levels as compared to the other samples ($p < 0.01$). Samples *Mmm* x *Mmd*-♀ (R6) and *Mmm* x *Mmd*-♂ (R7) showed similar expression levels ($p > 0.05$) that were approximately four times lower than that of the *Mmd*-♂ (R2) sample. The sample *Mmd*-♀ (R1) also yielded similar expression levels to the *Mmm* x *Mmd* hybrids (R6 and R7), but this was not supported with the p-values. The samples *Mmm*-♀ (R3), *Mmm*-♂ (R4), and *Mmd* x *Mmm*-♂ (R5) showed very similar expression levels ($p < 0.05$) that were between 1.2 and 1.7 times lower as compared to that of the control sample (Figure 2). Each of the hybrids yielded a similar expression pattern as compared to the paternal parent, so the hybrids showed parent-specific expression patterns within the *Mcts2* gene. Sample *Mmd*-♀ (R1) showed the greatest standard deviation of 1.33 while sample *Mmm* x *Mmd*-♂ (R7) yielded the smallest standard deviation of 0.29 (Figure 2). In looking at the raw C_t values observed within the *Mcts2* qRT-PCR experiment, sample *Mmd*-♀ (R1) showed the largest average C_t value of 31.78

(Table 14B). Samples *Mmd*-♂ (R2), *Mmm*-♀ (R3), *Mmm*-♂ (R4), *Mmd* x *Mmm*-♂ (R5), *Mmm* x *Mmd*-♀ (R6), and *Mmm* x *Mmd*-♂ (R7) yielded similar average C_t values between 26.72 and 29.48. The control sample (R8) showed the lowest C_t value of 23.84 (Table 14B).

Igf2r Gene

I observed that each sample showed increased expression in the *Igf2r* gene as compared to the control sample (Figure 3). The *Mmd*-♂ (R2), *Mmd* x *Mmm*-♂ (R5), and *Mmm* x *Mmd*-♀ (R6) samples had the largest increases in expression, and these samples had between 21.1 and 24.9 times greater *Igf2r* expression as compared to that of the control sample. The *Mmd*-♀ (R1) and *Mmm* x *Mmd*-♂ (R7) samples had similar levels of expression ($p > 0.05$) that were around 7 times lower than that of the *Mmd* x *Mmm*-♂ (R5) sample. The remaining two samples, which were the *Mmm* parental samples (R3 and R4), yielded similar expression levels, but this was not supported by the p-values (Figure 3). Sample *Mmd* x *Mmm*-♂ (R5) showed the greatest standard deviation of 6.44 while sample *Mmd*-♀ (R1) yielded the smallest standard deviation of 0.97 (Figure 3). In looking at the raw C_t values observed within the *Igf2r* qRT-PCR experiment, sample *Mmd*-♀ (R1) showed the largest average C_t value of 33.1 (Table 14C). Samples *Mmm*-♀ (R3) and *Mmm*-♂ (R4) yielded the lowest C_t value of 25.3 and 25.54 respectively. The samples *Mmd*-♂ (R2), *Mmd* x *Mmm*-♂ (R5), *Mmm* x *Mmd*-♀ (R6), *Mmm* x *Mmd*-♂ (R7), and the control (R8) showed similar average C_t values between 26.44 and 29.94 (Table 14C).

Nap1l5 Gene

I observed that each sample yielded increased expression in the *Nap1l5* gene as compared to the control sample (Figure 4). The *Mmd*-♂ (R2) sample had the largest increase in expression, and this sample had 80.2 times higher *Nap1l5* expression as compared to the expression of the control sample. Sample *Mmd*-♀ (R1) also showed 71.2 times higher *Nap1l5* expression (Figure 4). The expression levels of both of the *Mmd* parental samples (R1 and R2) were significantly different from that of the other samples ($p < 0.01$). Samples *Mmd* x *Mmm*-♂ (R5), *Mmm* x *Mmd*-♀ (R6), and *Mmm* x *Mmd*-♂ (R7) had similar expression levels ($p > 0.05$) that were over 10 times lower than that observed within the *Mmd*-♂ (R2) sample. Samples *Mmm*-♀ (R3) and *Mmm*-♂ (R4) showed expression levels 4 times lower than that of the *Mmd*-♂ (R2) sample (Figure 4). Each of the hybrids yielded lower levels of expression as compared to the parental subspecies, so the hybrids showed species-specific expression patterns within the *Nap1l5* genes. Sample *Mmd*-♂ (R2) had the greatest standard deviation of 29.53 while *Mmd* x *Mmm*-♂ (R5) showed the smallest standard deviation of 1.17 (Figure 4). In looking at the raw C_t values observed within the *Nap1l5* qRT-PCR experiment, *Mmd*-♀ (R1), *Mmd*-♂ (R2), *Mmd* x *Mmm*-♂ (R5), *Mmm* x *Mmd*-♀ (R6), and the control sample (R8) yielded average C_t values greater than 30 (Table 14D). Samples *Mmm*-♀ (R3), *Mmm*-♂ (R4), and *Mmm* x *Mmd*-♂ (R7) showed average C_t values between 26.8 and 29.1 (Table 14D).

Mest Gene

I observed that each sample yielded increased expression in the *Mest* gene as compared to the control sample (Figure 5). The *Mmd*-♂ (R2) sample had the largest increase in expression, and this sample had 18976 times higher *Mest* expression as

compared to the expression of the control sample. This sample had a significantly different expression level as compared to the other samples ($p < 0.01$). The *Mmd* x *Mmm*-♂ (R5) sample also had a significantly different expression level as compared to the other samples ($p < 0.01$). Samples *Mmm*-♀ (R3) and *Mmm*-♂ (R4) showed similar expression levels ($p > 0.05$) that were over 7 times lower than that observed within the *Mmd*-♂ (R2) sample. The samples *Mmd*-♀ (R1), *Mmm* x *Mmd*-♀ (R6), and *Mmm* x *Mmd*-♂ (R7) yielded very similar expression levels ($p > 0.05$) that were 240 and 600 times greater as compared to that of the control sample (Figure 5). Sample *Mmd*-♂ (R2) showed the greatest standard deviation of 4047.24 while sample *Mmd*-♀ (R1) yielded the smallest standard deviation of 53.76 (Figure 5). In looking at the raw C_t values observed within the *Mest* qRT-PCR experiment, the control sample (R8) showed the largest average C_t value of 31.17 (Table 14E). Samples *Mmd*-♀ (R1) and *Mmd*-♂ (R2) yielded similar average C_t values of 28.72 and 25.71. Samples *Mmm*-♀ (R3), *Mmm*-♂ (R4), *Mmd* x *Mmm*-♂ (R5), *Mmm* x *Mmd*-♀ (R6), and *Mmm* x *Mmd*-♂ (R7) showed similar average C_t values between 19.75 and 22.3 (Table 14E).

Discussion

Within the *H19*, *Igf2r*, and *Mest* genes, samples *Mmd*-♀ and *Mmm* x *Mmd*-♂ had very similar expression levels, which differed from nearly all the other samples ($p < 0.01$). These samples had the lowest level of expression within each of the genes. Within the *Mcts2* gene, samples *Mmd*-♀, *Mmd*-♂, *Mmm* x *Mmd*-♀, and *Mmm* x *Mmd*-♂ showed an increase in expression relative to the control, while the remaining samples had a similar decrease ($p > 0.05$). In terms of the *Nap1l5* gene, the *Mmd* parental samples yielded the greatest level of expression, while each of the hybrid samples showed similar

low levels ($p > 0.05$). Each gene had differences in expression between the hybrid and parental samples.

The hybrids experienced interesting, specific expression patterns within the *Mcts2* and *Nap1l5* genes. Within the *Nap1l5* genes, each of the hybrids experienced similar levels of expression that were significantly lower than that of both parental subspecies. Thus, the hybrids experienced species-specific expression patterns within the *Nap1l5* gene. Within the *Mcts2* gene, each of the hybrids experienced a similar expression pattern as compared to the paternal parent. The hybrids within this gene showed parent-specific expression patterns. These expression patterns suggest that there are disruptions in the *Mcts2* and *Nap1l5* genes within the parental subspecies.

Within each gene, those samples that yielded differing expression levels as compared to the other samples may have possibly experienced disruption in DNA methylation patterns. DNA methylation within the promoters of genes can cause changes in the structure of the DNA molecule, which can prevent gene expression (Das and Singal, 2004; Jones and Takai, 2001). Those samples, such as frequently *Mmd*-♂, which showed a higher expression level as compared to the other samples, possibly have less methylation than the remaining samples. However, those samples, often *Mmd*-♀ and *Mmm* x *Mmd*-♂, which experienced a smaller expression level as compared to the other samples, possibly have greater methylation than the other samples. I have analyzed the methylation patterns of the *Mcts2* and *Nap1l5* genes within adult tissues of the *Mmd* and *Mmm* parental subspecies as well as their hybrids. In terms of the *Mcts2* gene, the samples *Mmd*-♂, *Mmd*-♀, and *Mmm* x *Mmd*-♀ showed a decrease of methylation, which corresponded to an increase in expression within the corresponding samples as compared

to the other samples. The *Mmm*-♀ sample also yielded a decrease in methylation; however, instead of an increase in expression, this sample showed a decrease as compared to the other samples. This suggests that the changes in expression observed within the samples *Mmm* x *Mmd*-♂, *Mmm*-♀, *Mmd* x *Mmm*-♂, and *Mmm*-♂ were not related to methylation changes. In terms of the *Nap1l5* gene, the samples *Mmd*-♂, *Mmm*-♂, *Mmm*-♀, and *Mmm* x *Mmd*-♀ yielded an increase in methylation which should have corresponded to a decrease in expression. However, I observed that each sample showed an increase in expression relative to the adult control. Within each gene, there were differences between the expression levels of the parental and hybrid samples.

Previous studies have shown that differences in the expression levels of imprinted genes are present in mouse hybrids of the *Mus* genus. In *Mus musculus* and *Mus spretus* hybrids, researchers discovered that the imprinted *Peg1*, *Peg3*, and *Snrpn* genes showed a loss of imprinting and experienced biallelic expression (Shi et al., 2004, 2005). Researchers discovered that there was aberrant over-expression of X-linked retroelements within *Mus musculus* and *Mus caroli* hybrids (Brown et al., 2008, 2012). Studies have also shown that within the *M. m. musculus* CzechII/Ei and *M. m. domesticus* hybrids there were no disruptions within the expression of the *Igf2r* and *CdknI2* genes (Hagan et al., 2004).

As my control sample, I used genetic material isolated from the livers of adult mice. Differential expression is observed between adult mice and mice embryos. The expression of *Mest* and *H19* is down-regulated in adult samples (Bartolomei et al., 1991; Nishita et al., 1999; Rajabpour-Niknam et al., 2013). The use of this control explains the large fold changes observed in the *Mest* gene results. This pattern of expression suggests

that the adult samples may have not been the most ideal control for this experiment. However, I was interested in comparing the relative expression levels across the samples.

Genetic expression levels of imprinted genes have been found to vary among individuals. This individual variation was observed in studies which examined *Mus musculus* and *Mus spretus* hybrids. These studies showed that only a percentage of tissues examined yielded an increase in the expression of the *Peg1*, *Peg3*, and *Snrpn* imprinted genes (Shi et al., 2004, 2005). Therefore, the differences in expression observed within this experiment may be due to individual variation.

Reproductive isolation, which can be created as genetic differences accumulate between populations, can lead to speciation (Good et al., 2008a, 2008b; Palumbi, 1994; Turner et al., 2012). The linkage between genetic variation and speciation is not fully understood within the *Mmm* and *Mmd* subspecies. However, genetic differences leading to reproductive isolation have been observed within genes, such as the *Prdm9* gene, involved in growth and development (Bhattacharyya et al., 2013; Flachs et al., 2012, 2014; Geraldes et al., 2011; Mihola et al., 2009; Palumbi, 1994). Each of the genes examined are very important in growth and development. The hybrids showed parent-specific and species-specific expression patterns within the *Mcts2* and *Nap1l5* genes. These data suggest that there are genetic differences within the *Mcts2* and *Nap1l5* genes that potentially contribute to the reproductive isolation and speciation of the *Mmm* and *Mmd* organisms. The differences observed between males and females suggests that there is variation between individuals. The *H19* and *Igf2r* genes are maternally expressed while the other three genes are paternally expressed. Because all of the genes yielded expression levels that differed between the parents and hybrids, there does not appear to

be an association between the maternal/paternal imprinting pattern and the expression levels. Because each of the genes have similar functions, there is not a clear association between gene functions and expression levels. In the future, I feel more parental and hybrid samples should be examined to determine if individual variation had been observed.

Table 13. Primers used in Real-Time PCR. A description of the primers used in real-time PCR. The name of the primers, the name of the gene associated with the primers, and the primer sequences are listed here. The primer sequences were obtained and designed through PrimerBank and IDT PrimeTime® (PrimeTime® program, 2015; Spandidos et al., 2008, 2010; Wang and Seed, 2003). Each of the primer sets were tested for efficiency, and they all had efficiencies between 89% and 110% and $R^2 > 0.900$. The chromosome position and coding sequence position were found within the UCSC Genome Browser under Build 37 (Kent et al., 2002).

Gene	Chromosome Location and Position of Coding Sequence (bp)	Primer Name	Primer Sequence
H19	Chromosome 7; 149762966 – 149763364	Mm.PT.58.5167014	GTAGCCTCCGTATTTAGCATCC
			TGCCTTGTGAATATCTCTCCTTG
Mcts2	Chromosome 2; 152513007 – 152513552	Mcts2-F1	GAGAAGGAAAGTGTGTCCAACTG
		Mcts2-R1	ATTAAGCCACGGCTCGATACC
Nap1l5	Chromosome 6; 58856491 – 58856961	Mm.PT.58.41249674.g	CTGGTGTAGTGTGATGAATGGA
			CTGTGAGAACTGGACTTGAGAC
Igf2r	Chromosome 17; 12876576 – 12962399	Igf2r-3-F	AGCTAAATGGTGGCTATCTGGT
		Igf2r-3-R	GGGTCGGCCAACGTCAAAT
eEF-2	Chromosome 10; 80639472 – 80644827	eEF-2-PB-1-F	CCGACTCCCTTGTGTGCAA
		eEF-2-PB-1-R	AGTTCAGGTCGTTCTCAGAGAG
Mest	Chromosome 6; 30688310 – 30697169	Mm.PT.58.29129569	GAAAGCACACCTCCGTCTT
			GCTCACCATAAAGAGTCTCTGTC

Table 14. Raw Real-Time PCR Data. Raw real-time PCR data for each of the 7 samples (R1-R7) and the control sample (R8). For every reaction, each sample was run in triplicate and the average C_t values are shown here. Data for five reactions are shown and separate primers were used in each of these reactions to amplify a section of the coding regions of the *H19* (A), *Mcts2* (B), *Igf2r* (C), *Nap1l5* (D), and *Mest* (E) genes.

A:

Sample	Avg. Ct
R1	34.95
R2	31.42
R3	26.76
R4	26.57
R5	28.77
R6	28.98
R7	28.34
R8	23.17

B:

Sample	Avg. Ct
R1	31.78
R2	29.48
R3	27.05
R4	27.15
R5	28.78
R6	28.42
R7	26.72
R8	23.84

C:

Sample	Avg. Ct
R1	33.1
R2	29.94
R3	25.3
R4	25.54
R5	26.44
R6	26.91
R7	28.17
R8	29.76

D:

Sample	Avg. Ct
R1	30.87
R2	30.14
R3	27.58
R4	26.83
R5	32.04
R6	31.36
R7	29.1
R8	31.89

E:

Sample	Avg. Ct
R1	28.72
R2	25.71
R3	20.37
R4	19.75
R5	20.69
R6	21.78
R7	22.3
R8	31.17

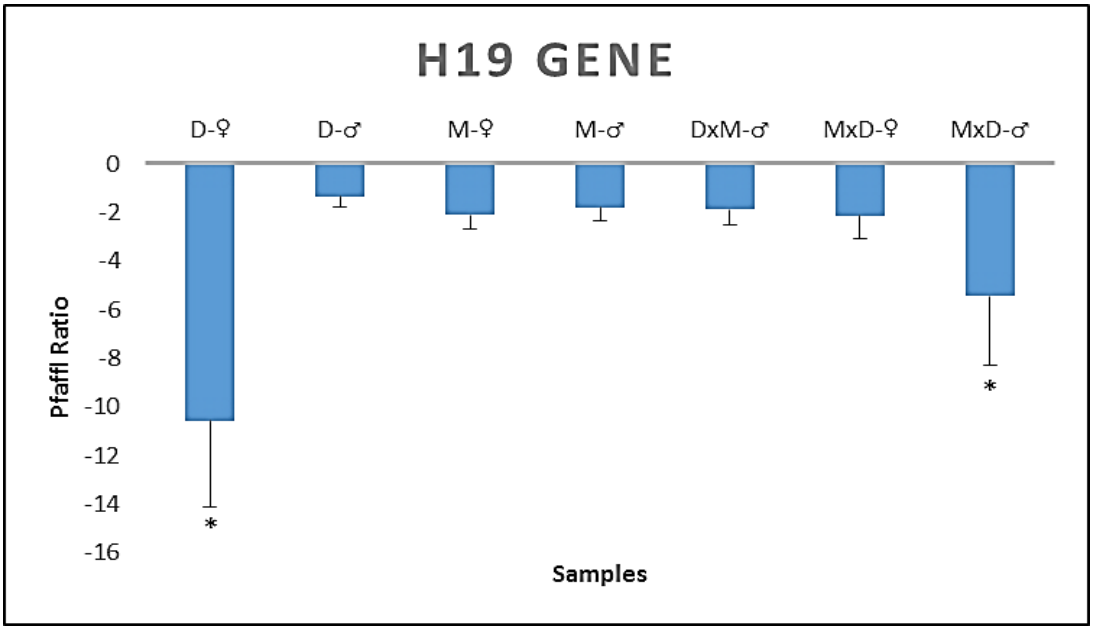

Figure 1. Normalized Real-Time PCR Data for the *H19* Gene. Normalized real-time PCR data for each of the 7 samples (R1-R7). The raw C_t values produced during qPCR were normalized through the Pfaffl method to produce the Pfaffl ratio, which is a fold increase or decrease in expression. Each sample was run in triplicate. Primers were used in this reaction to amplify a section of the coding region of the *H19* gene. Standard deviation bars are shown. The (*) indicates that the Pfaffl ratios of those samples are significantly different from that of all the other samples ($p < 0.01$).

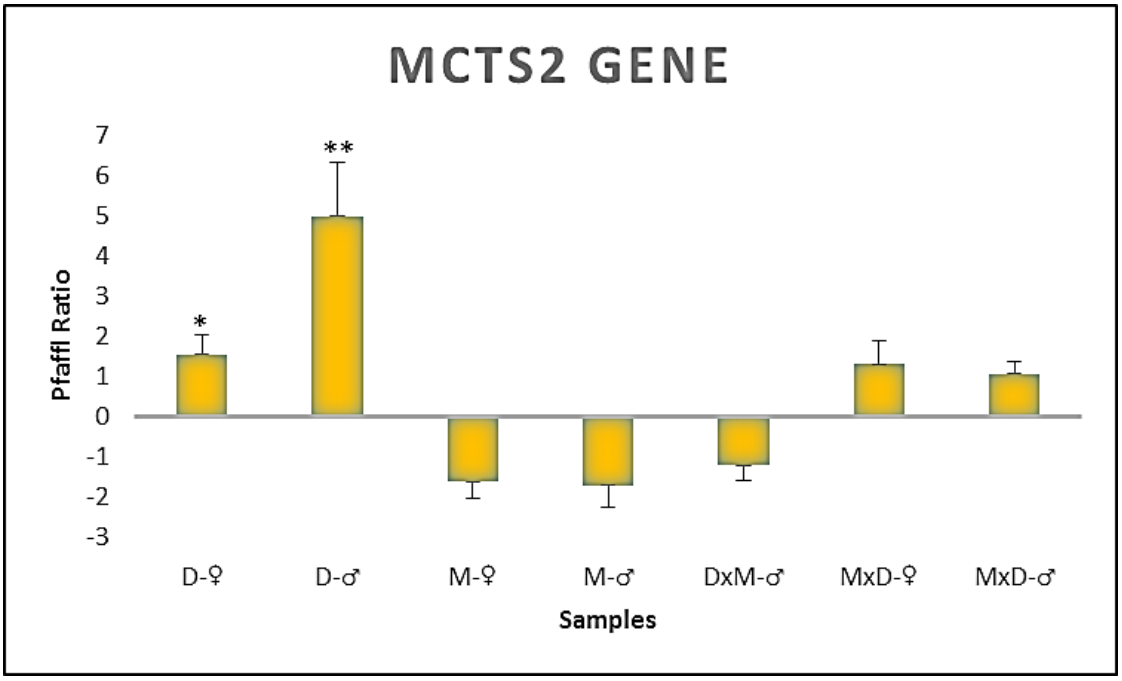

Figure 2. Normalized Real-Time PCR Data for the *Mcts2* Gene. Normalized real-time PCR data for each of the 7 samples (R1-R7). The raw C_t values produced during qPCR were normalized through the Pfaffl method to produce the Pfaffl ratio, which is a fold increase or decrease in expression. Each sample was run in triplicate. Primers were used in this reaction to amplify a section of the coding region of the *Mcts2* gene. Standard deviation bars are shown. The (*) indicates that the Pfaffl ratio of that sample is significantly different from that of all the other samples ($p < 0.05$), while the (**) also indicates that the ratio is significantly different from that of all the other samples ($p < 0.01$).

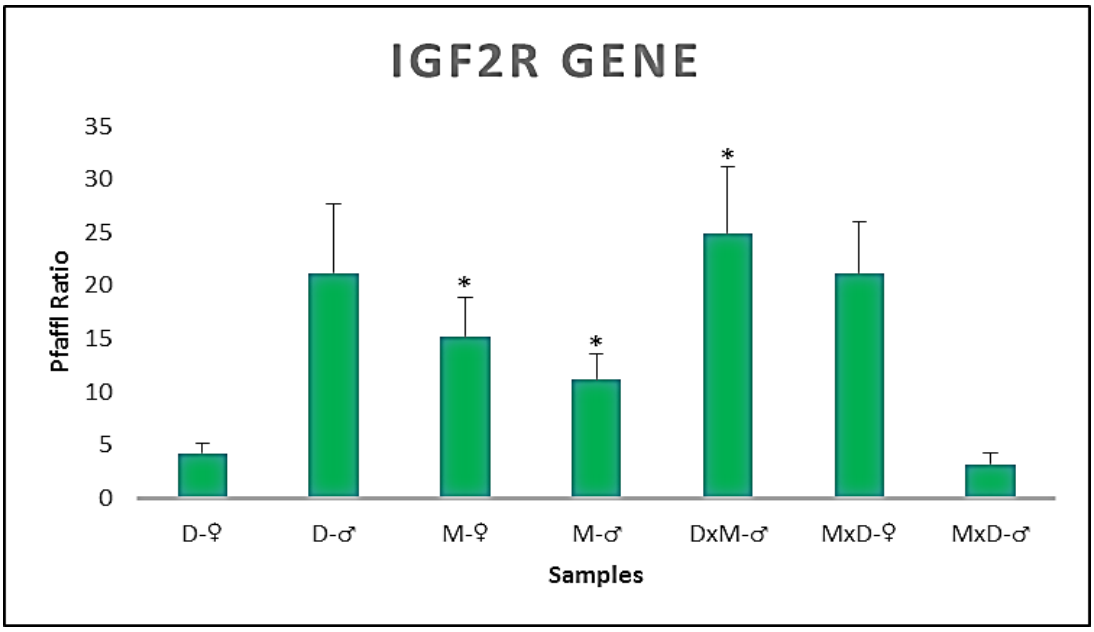

Figure 3. Normalized Real-Time PCR Data for the *Igf2r* Gene. Normalized real-time PCR data for each of the 7 samples (R1-R7). The raw C_t values produced during qPCR were normalized through the Pfaffl method to produce the Pfaffl ratio, which is a fold increase or decrease in expression. Each sample was run in triplicate. Primers were used in this reaction to amplify a section of the coding region of the *Igf2r* gene. Standard deviation bars are shown. The (*) indicates that the Pfaffl ratios of those samples are significantly different from that of all the other samples ($p < 0.01$).

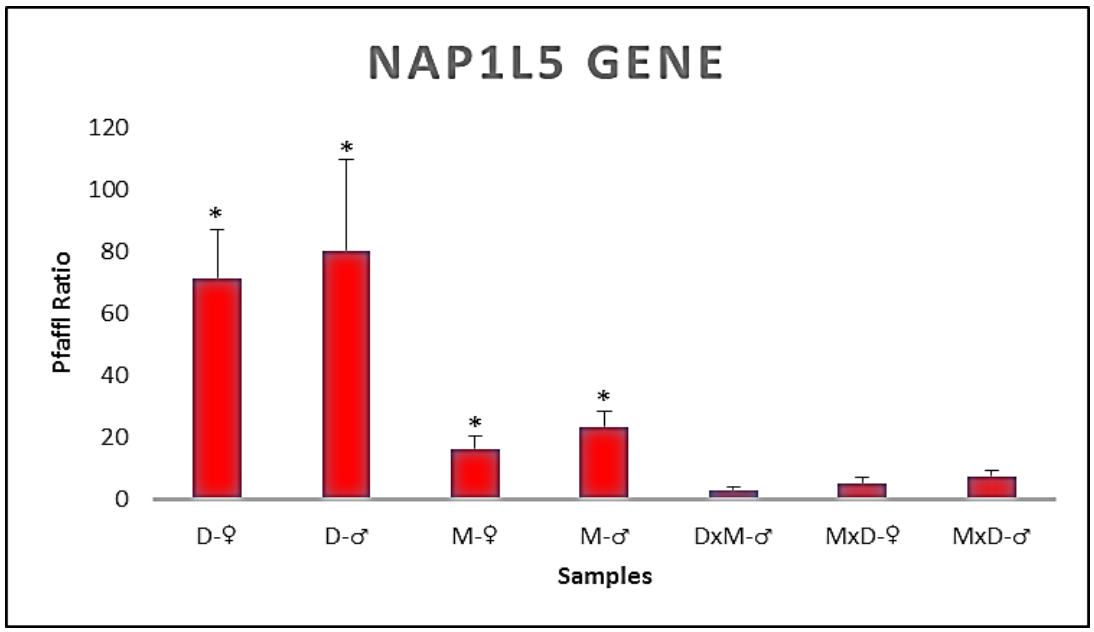

Figure 4. Normalized Real-Time PCR Data for the *Nap1l5* Gene. Normalized real-time PCR data for each of the 7 samples (R1-R7). The raw C_t values produced during qPCR were normalized through the Pfaffl method to produce the Pfaffl ratio, which is a fold increase or decrease in expression. Each sample was run in triplicate. Primers were used in this reaction to amplify a section of the coding region of the *Nap1l5* gene. Standard deviation bars are shown. The (*) indicates that the Pfaffl ratios of those samples are significantly different from that of all the other samples ($p < 0.01$).

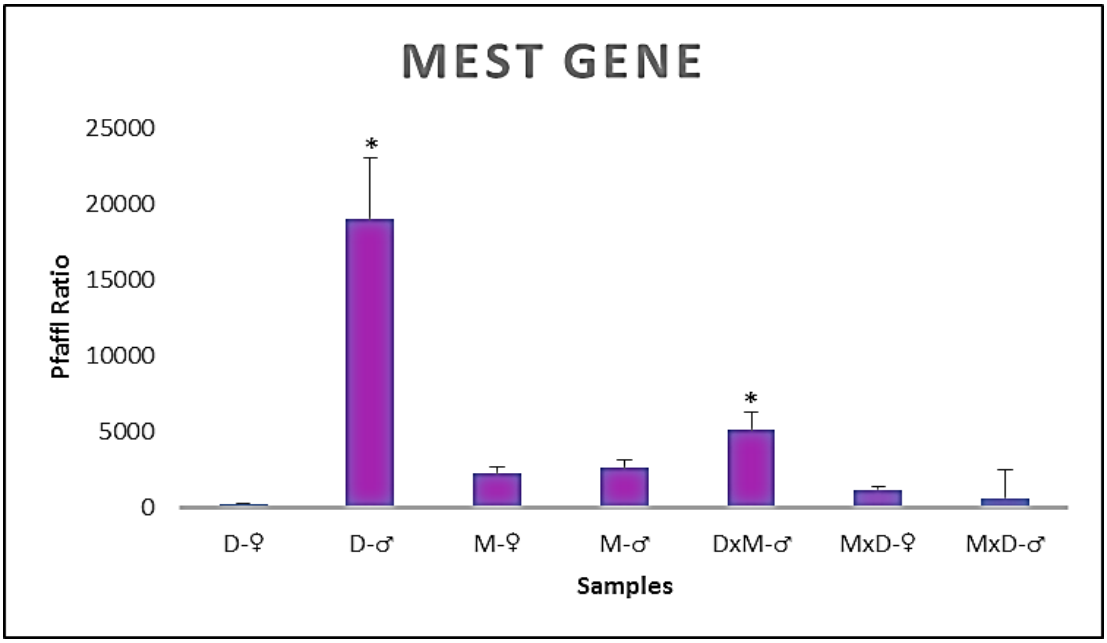

Figure 5. Normalized Real-Time PCR Data for the *Mest* Gene. Normalized real-time PCR data for each of the 7 samples (R1-R7). The raw C_t values produced during qPCR were normalized through the Pfaffl method to produce the Pfaffl ratio, which is a fold increase or decrease in expression. Each sample was run in triplicate. Primers were used in this reaction to amplify a section of the coding region of the *Mest* gene. Standard deviation bars are shown. The (*) indicates that the Pfaffl ratios of those samples are significantly different from that of all the other samples ($p < 0.01$).

SUMMARY AND CONCLUSIONS

In the first portion of my experiment, I analyzed the methylation status of DMDs associated with imprinted genes within *M. m. musculus*, *M. m. domesticus*, and their hybrids. I performed this analysis in order to determine if the methylation patterns within these regions differed within the hybrids. I modified the DNA of the parental samples and their hybrids with bisulfite. I amplified a section of the DMD of five genes. I cloned these products and sequenced them. The genes I examined were *Mcts2*, *Nap1l5*, *Peg10*, *Zac1*, and *Zim2*. I observed that each gene showed disruption in methylation relative to the expectation that only one allele would be methylated. Within each of the genes, except *Mcts2*, *Peg10*, and *Zim2*, I observed disruption in the methylation patterns of the hybrids. There was also disruption in methylation within the parental samples for each gene except *Zac1*. Both decreases and increases of methylation were observed for the examined genes. Loss of methylation has been observed within the hybrids of the *Mus* genus and within patients with diabetes mellitus (Arima et al., 2006; Battulin et al., 2009; Brown et al., 2008, 2012). Gain of methylation within genes, such as transcription factors, has also been discovered to be associated with cancers (Arima et al., 2006). Within this experiment, the parental subspecies yielded a total of five increases in methylation and three decreases. The hybrid organisms showed a total of one increase in methylation and four decreases. The *Nap1l5* gene yielded the greatest number of disruption events. These methylation changes may lead to altered gene expression levels in hybrids.

In the next portion of my experiment, I measured the gene expression difference between *M. m. musculus*, *M. m. domesticus*, and their hybrids. I isolated the RNA of the parental samples, three of their hybrids, and a control sample. I synthesized cDNA from the RNA. I performed real-time PCR using these samples with primers for five test genes and one control, housekeeping gene (*eEF-2*). The primers amplified a portion of the coding region (transcript). The genes I examined were *H19, Igf2r, Mcts2, Mest,* and *Nap1l5*. I normalized the resulting C_t values using the Pfaffl method (Pfaffl, 2001). I normalized the data with the control sample and relative to the housekeeping gene, *eEF-2*. I observed that each gene yielded differences in the expression levels of the parental and hybrid samples. Changes in the expression of imprinted genes have been observed within other hybrids of the *Mus* genus (Shi et al., 2004, 2005). Within the *H19*, *Igf2r*, and *Mest* genes, one parental (*Mmd*-♀) sample and one hybrid (*Mmm* x *Mmd*-♂) sample experienced the smallest expression level as compared to the other samples. The *Mmd* parental samples as well as the *Mmm* x *Mmd* hybrid samples showed an increase in *Mcts2* expression as compared to the control. The other samples yielded a decrease in *Mcts2* expression. Within the *Mcts2* gene, the hybrids showed parent-specific expression patterns. Within the *Nap1l5* gene, each of the hybrid samples had the lowest level of expression as compared to the other samples. The hybrids showed species-specific expression patterns within the *Nap1l5* gene. These results suggest that genetic variation within the *Mcts2* and *Nap1l5* genes can contribute to hybrid inviability and thus reproductive isolation within the subspecies examined (Geraldes et al., 2011; Palumbi, 1994).

It is known that the accumulation of genetic differences can lead to reproductive isolation and thus speciation. The linkage between genetic variation and speciation is not fully understood within the separate subspecies *M. m. musculus* and *M. m. domesticus* (Geraldes et al., 2011; Palumbi, 1994). Genetic differences leading to reproductive isolation have been observed within genes associated with growth and development (Good et al., 2008a, 2008b; Turner et al., 2012). Each of the eight genes examined are important in growth and development. Parent-specific and species-specific expression differences were observed for the *Mcts2* and *Nap1l5* genes within the hybrids. This data suggests that these two genes were potentially involved in the reproductive isolation and speciation of the *M. m. musculus* and *M. m. domesticus* subspecies.

In the future, I believe more parental and hybrid samples should be examined in order to determine if individual variation had been observed. I think more maternally expressed genes should be examined to determine if there is a pattern observed between the genomic imprinting patterns and the expression or methylation patterns within hybrids. By doing so, a relevant link between the genomic imprinting pattern of a gene and the gene's potential involvement in the speciation of the house mouse subspecies could be determined. I also believe the methylation patterns of the *H19, Mest*, and *Igf2r* genes should be examined to determine if the expression changes observed are associated with the methylation patterns. Finally, I feel the expression patterns of the *Peg10, Zac1*, and *Zim2* genes should be examined to determine if the changes in methylation observed are involved in the expression patterns.

REFERENCES

Altschul, S.F., Gish, W., Miller, W., Myers, E.W., and Lipman, D.J. (1990). Basic local alignment search tool. J. Mol. Biol. *215*, 403–410.

Arima, T., Yamasaki, K., John, R.M., Kato, K., Sakumi, K., Nakabeppu, Y., Wake, N., and Kono, T. (2006). The human HYMAI/PLAGL1 differentially methylated region acts as an imprint control region in mice. Genomics *88*, 650–658.

Ashbrook, D.G., and Hager, R. (2013). Empirical testing of hypotheses about the evolution of genomic imprinting in mammals. Front. Neuroanat. *7*, 6.

Bartolomei, M.S., Zemel, S., and Tilghman, S.M. (1991). Parental Imprinting of the Mouse H19 Gene. Nature *351*, 153–155.

Battulin, N.R., Pristyazhnyuk, I.E., Matveeva, N.M., Fishman, V.S., Vasilkova, A.A., and Serov, O.L. (2009). Allelic expression and DNA methylation profiles of promoters at the parental Oct4 and Nanog genes in Mus musculus ES cell/Mus caroli splenocyte hybrid cells. Cell Tissue Res. *337*, 439–448.

Bhattacharyya, T., Gregorova, S., Mihola, O., Anger, M., Sebestova, J., Denny, P., Simecek, P., and Forejt, J. (2013). Mechanistic basis of infertility of mouse intersubspecific hybrids. Proc. Natl. Acad. Sci. U. S. A. *110*, E468–E477.

Birger, Y., Shemer, R., Park, J., and Razin, A. (1999). The imprinting box of the mouse Igf2r gene. Nature *397*, 84–88.

Božíková, E., Munclinger, P., Teeter, K.C., Tucker, P.K., Macholán, M., and Piálek, J. (2005). Mitochondrial DNA in the hybrid zone between Mus musculus and Mus musculus domesticus: a comparison of two transects. Biol. J. Linn. Soc. *84*, 363–378.

Brannan, C.I., Dees, E.C., Ingram, R.S., and Tilghman, S.M. (1990). The product of the H19 gene may function as an RNA. Mol. Cell. Biol. *10*, 28–36.

Brown, J.D., Golden, D., and O'Neill, R.J. (2008). Methylation perturbations in retroelements within the genome of a Mus interspecific hybrid correlate with double minute chromosome formation. Genomics *91*, 267–273.

Brown, J.D., Piccuillo, V., and O'Neill, R.J. (2012). Retroelement demethylation associated with abnormal placentation in mus musculus × mus caroli hybrids. Biol. Reprod. *86*, 88.

Burt, A., and Trivers, R. (1998). Genetic Conflicts in Genomic Imprinting. Proc. R. Soc. Lond. B Biol. Sci. *265*, 2393–2397.

Choufani, S., Shapiro, J.S., Susiarjo, M., Butcher, D.T., Grafodatskaya, D., Lou, Y., Ferreira, J.C., Pinto, D., Scherer, S.W., Shaffer, L.G., et al. (2011). A novel approach identifies new differentially methylated regions (DMRs) associated with imprinted genes. Genome Res. *21*, 465–476.

Cowley, M., Wood, A.J., Böhm, S., Schulz, R., and Oakey, R.J. (2012). Epigenetic control of alternative mRNA processing at the imprinted Herc3/Nap1l5 locus. Nucleic Acids Res. *40*, 8917–8926.

Daniel, G., Schmidt-Edelkraut, U., Spengler, D., and Hoffmann, A. (2015). Imprinted Zac1 in neural stem cells. World J. Stem Cells *7*, 300–314.

Das, P.M., and Singal, R. (2004). DNA Methylation and Cancer. J. Clin. Oncol. *22*, 4632–4642.

Day, T., and Bonduriansky, R. (2004). Intralocus sexual conflict can drive the evolution of genomic imprinting. Genetics *167*, 1537–1546.

Dong, C., Hu, A., Ni, Y., Zuo, Y., and Li, G.H. (2013). Effects of midazolam, pentobarbital and ketamine on the mRNA expression of ion channels in a model organism Daphnia pulex. BMC Anesthesiol. *13*, 32.

Du, X., Ounissi-Benkalha, H., Loder, M.K., Rutter, G.A., and Polychronakos, C. (2012). Overexpression of ZAC impairs glucose-stimulated insulin translation and secretion in clonal pancreatic beta-cells. Diabetes Metab. Res. Rev. *28*, 645–653.

Edwards, C.A., and Ferguson-Smith, A.C. (2007). Mechanisms regulating imprinted genes in clusters. Curr. Opin. Cell Biol. *19*, 281–289.

Ferguson-Smith, A.C., Sasaki, H., Cattanach, B.M., and Surani, M.A. (1993). Parental-origin-specific epigenetic modification of the mouse H19 gene. Nature *362*, 751–755.

Flachs, P., Mihola, O., Simeček, P., Gregorová, S., Schimenti, J.C., Matsui, Y., Baudat, F., de Massy, B., Piálek, J., Forejt, J., et al. (2012). Interallelic and intergenic incompatibilities of the Prdm9 (Hst1) gene in mouse hybrid sterility. PLoS Genet. *8*, e1003044.

Flachs, P., Bhattacharyya, T., Mihola, O., Piálek, J., Forejt, J., and Trachtulec, Z. (2014). Prdm9 incompatibility controls oligospermia and delayed fertility but no selfish transmission in mouse intersubspecific hybrids. PloS One *9*, e95806.

Geraldes, A., Basset, P., Smith, K.L., and Nachman, M.W. (2011). Higher differentiation among subspecies of the house mouse (Mus musculus) in genomic regions with low recombination. Mol. Ecol. *20*, 4722–4736.

Good, J.M., Handel, M.A., Nachman, M.W., and Feder, J. (2008a). Asymmetry and polymorphism of hybrid male sterility during the early stages of speciation in house mice. Evolution *62*, 50–65.

Good, J.M., Dean, M.D., and Nachman, M.W. (2008b). A complex genetic basis to x-linked hybrid male sterility between two species of house mice. Genetics *179*, 2213–2228.

Gos, M. (2013). Epigenetic mechanisms of gene expression regulation in neurological diseases. Acta Neurobiol. Exp. (Warsz.) *73*, 19–37.

Gregg, C., Zhang, J., Weissbourd, B., Luo, S., Schroth, G.P., Haig, D., and Dulac, C. (2010). High-resolution analysis of parent-of-origin allelic expression in the mouse brain. Science *329*, 643–648.

Gu, T., Zhao, S.-H., and Li, C.-C. (2011). NAP1L5 is imprinted in porcine placenta. Anim. Genet. *42*, 568–569.

Hagan, J.P., Kozlov, S.V., Chiang, Y.S., Sewell, L., and Stewart, C.L. (2004). Intraspecific mating with CzechII/Ei mice rescue lethality associated with loss of function mutations of the imprinted genes, Igf2r and Cdkn1c. Genomics *84*, 836–843.

Haig, D. (2000). The kinship theory of genomic imprinting. Annu. Rev. Ecol. Syst. 9–32.

Haig, D. (2004). Genomic Imprinting and Kinship: How Good is the Evidence? Annu. Rev. Genet. *38*, 553–585.

Harada, H., Nagai, H., Ezura, Y., Yokota, T., Ohsawa, I., Yamaguchi, K., Ohue, C., Tsuneizumi, M., Mikami, I., Terada, Y., et al. (2002). Down-regulation of a novel gene, DRLM, in human liver malignancy from 4q22 that encodes a NAP-like protein. Gene *296*, 171–177.

Hino, T., Inoue, K., Ishino, F., Kaneko-Ishino, T., Kohda, T., Miki, H., Nakamura, K., Naruse, M., Ogonuki, N., Ogura, A., et al. (2006). Deletion of Peg10, an imprinted gene acquired from a retrotransposon, causes early embryonic lethality. Nat. Genet. *38*, 101+.

Hishida, T., Naito, K., Osada, S., Nishizuka, M., and Imagawa, M. (2007). peg10, an imprinted gene, plays a crucial role in adipocyte differentiation. FEBS Lett. *581*, 4272–4278.

Huang, Z., Han, Z., Zhang, F., He, H., Yu, S., and Wu, Q. (2014). Spatiotemporal expression of retrogene–host pair Mcts2/H13 in mouse embryo, and Mcts2 has no influence on H13 transcription pattern in NIH/3T3 cells. Acta Histochem. *116*, 312–318.

Huntriss, J.D., Hemmings, K.E., Hinkins, M., Rutherford, A.J., Sturmey, R.G., Elder, K., and Picton, H.M. (2013). Variable imprinting of the MEST gene in human preimplantation embryos. Eur. J. Hum. Genet. *21*, 40–47.

Hutter, B., Bieg, M., Helms, V., and Paulsen, M. (2010a). Divergence of imprinted genes during mammalian evolution. BMC Evol. Biol. *10*, 116.

Hutter, B., Bieg, M., Helms, V., and Paulsen, M. (2010b). Imprinted genes show unique patterns of sequence conservation. BMC Genomics *11*, 649.

Hutter, B., Bieg, M., Helms, V., and Paulsen, M. (2010c). Conserved elements in imprinted genes. New Biotechnol. *27, Supplement 1*, S69.

Ineson, J., Stayner, C., Hazlett, J., Slobbe, L., Robson, E., Legge, M., and Eccles, M.R. (2012). Somatic reactivation of expression of the silent maternal Mest allele and acquisition of normal reproductive behaviour in a colony of Peg1/Mest mutant mice. J. Reprod. Dev. *58*, 490–500.

Janoušek, V., Wang, L., Luzynski, K., Dufková, P., Vyskočilová, M.M., Nachman, M.W., Munclinger, P., Macholán, M., Piálek, J., and Tucker, P.K. (2012). Genome-wide architecture of reproductive isolation in a naturally occurring hybrid zone between Mus musculus musculus and M. m. domesticus. Mol. Ecol. *21*, 3032–3047.

Jones, P.A., and Takai, D. (2001). The role of DNA methylation in mammalian epigenetics. Science *293*, 1068–1070.

Kearse, M., Moir, R., Wilson, A., Stones-Havas, S., Cheung, M., Sturrock, S., Buxton, S., Cooper, A., Markowitz, S., Duran, C., Thierer, T., Ashton, B., Mentjies, P., & Drummond, A. (2012). Geneious Basic: an integrated and extendable desktop software platform for the organization and analysis of sequence data. Bioinformatics *28*, 1647-1649.

Kent, W.J., Sugnet, C.W., Furey, T.S., Roskin, K.M., Pringle, T.H., Zahler, A.M., and Haussler, and D. (2002). The Human Genome Browser at UCSC. Genome Res. *12*, 996–1006.

Kim, J., Bergmann, A., and Stubbs, L. (2000). Exon Sharing of a Novel Human Zinc-Finger Gene, ZIM2, and Paternally Expressed Gene 3 (PEG3). Genomics *64*, 114–118.

Kim, J., Bergmann, A., Lucas, S., Stone, R., and Stubbs, L. (2004). Lineage-specific imprinting and evolution of the zinc-finger gene ZIM2. Genomics *84*, 47–58.

Kramer, C.Y. (1956). Extension of Multiple Range Tests to Group Means with Unequal Numbers of Replications. Biometrics *12*, 307–310.

Kropáčková, L., Piálek, J., Gergelits, V., Forejt, J., and Reifová, R. (2015). Maternal-fetal

genomic conflict and speciation: no evidence for hybrid placental dysplasia in crosses between two house mouse subspecies. J. Evol. Biol. n/a – n/a.

Lucifero, D., Mertineit, C., Clarke, H.J., Bestor, T.H., and Trasler, J.M. (2002). Methylation Dynamics of Imprinted Genes in Mouse Germ Cells. Genomics *79*, 530–538.

Machado, A., de Souza, W., de Pádua, M., da Silva Rodrigues Machado, A., and Figueiredo, L. (2013). Development of a One-Step SYBR Green I Real-Time RT-PCR Assay for the Detection and Quantitation of Araraquara and Rio Mamore Hantavirus. Viruses *5*, 2272–2281.

Mayer, W., Hemberger, M., Frank, H.-G., Grümmer, R., Winterhager, E., Kaufmann, P., and Fundele, R. (2000). Expression of the imprinted genes MEST/Mest in human and murine placenta suggests a role in angiogenesis. Dev. Dyn. *217*, 1–10.

Mihola, O., Trachtulec, Z., Vlcek, C., Schimenti, J.C., and Forejt, J. (2009). A mouse speciation gene encodes a meiotic histone H3 methyltransferase. Science *323*, 373–375.

Morison, I.M., Ramsay, J.P., and Spencer, H.G. (2005). A census of mammalian imprinting. Trends Genet. TIG *21*, 457–465.

Nishita, Y., Sado, T., Yoshida, I., and Takagi, N. (1999). Effect of CpG methylation on expression of the mouse imprinted gene Mest. Gene *226*, 199–209.

Oka, A., Aoto, T., Totsuka, Y., Takahashi, R., Ueda, M., Mita, A., Sakurai-Yamatani, N., Yamamoto, H., Kuriki, S., and Takagi, N. (2007). Disruption of genetic interaction between two autosomal regions and the X chromosome causes reproductive isolation between mouse strains derived from different subspecies. Genetics *175*, 185.

Ono, R., Kobayashi, S., Wagatsuma, H., Aisaka, K., Kohda, T., Kaneko-Ishino, T., and Ishino, F. (2001). A Retrotransposon-Derived Gene, PEG10, Is a Novel Imprinted Gene Located on Human Chromosome 7q21. Genomics *73*, 232–237.

Palumbi, S.R. (1994). Genetic Divergence, Reproductive Isolation, and Marine Speciation. Annu. Rev. Ecol. Syst. *25*, 547–572.

Pfaffl, M.W. (2001). A new mathematical model for relative quantification in real-time RT–PCR. Nucleic Acids Res. *29*, e45.

Phadnis, N., and Orr, H.A. (2009). A single gene causes both male sterility and segregation distortion in Drosophila hybrids. Science *323*, 376.

PrimeTime® program, IDT, Coralville, USA. Retrieved 2015. http://www.idtdna.com/Scitools.

Rachmilewitz, J., Goshen, R., Ariel, I., Schneider, T., de Groot, N., and Hochberg, A. (1992). Parental imprinting of the human H19 gene. FEBS Lett. *309*, 25–28.

Rainier, S., Johnson, L.A., Dubry, C.J., Ping, A.J., Grundy, P.E., Feinberg, A.P. (1993). Relaxation of imprinted genes in human cancer. Nature *362*, 747.

Rajabi-Maham, H., Orth, A., and Bonhomme, F. (2008). Phylogeography and postglacial expansion of Mus musculus domesticus inferred from mitochondrial DNA coalescent, from Iran to Europe. Mol. Ecol. *17*, 627–641.

Rajabpour-Niknam, M., Totonchi, M., Shahhosseini, M., Farrokhi, A., Alipour, H., and Eftekhari-Yazdi, P. (2013). Quantitative expression of developmental genes, Pou5f1 (Oct4) and Mest (Peg1), in vitrified mouse embryos. Iran. J. Reprod. Med. *11*, 733–740.

Reinhart, B., Eljanne, M., and Chaillet, J.R. (2002). Shared Role for Differentially Methylated Domains of Imprinted Genes. Mol. Cell. Biol. *22*, 2089–2098.

Reinhart, B., Paoloni-Giacobino, A., and Chaillet, J.R. (2006). Specific Differentially Methylated Domain Sequences Direct the Maintenance of Methylation at Imprinted Genes. Mol. Cell. Biol. *26*, 8347–8356.

Reis, M.B., Ramos, P.M., Camargo, J.L., and Rainho, C.A. (2013). Analysis of the DNA methylation of the H19 gene in human bladder cancer. BMC Proc. *7*, P47.

Renfree, M.B., Suzuki, S., and Kaneko-Ishino, T. (2013). The origin and evolution of genomic imprinting and viviparity in mammals. Philos. Trans. R. Soc. B Biol. Sci. *368*.

Del Rio, T., Fossella, J.A., Matteson, P., O'Neill, M.J., Tilghman, S.M., and Vrana, P.B. (2000). Genetic and epigenetic incompatibilities underlie hybrid dysgenesis in Peromyscus. Nat. Genet. *25*, 120+.

Schulz, R., Woodfine, K., Menheniott, T.R., Bourc'his, D., Bestor, T., and Oakey, R.J. (2008). WAMIDEX: a web atlas of murine genomic imprinting and differential expression. Epigenetics Off. J. DNA Methylation Soc. *3*, 89–96.

Schütt, S., Florl, A.R., Shi, W., Hemberger, M., Orth, A., Otto, S., Schulz, W.A., and Fundele, R.H. (2003). DNA methylation in placentas of interspecies mouse hybrids. Genetics *165*, 223–228.

Shi, W., Lefebvre, L., Yu, Y., Otto, S., Krella, A., Orth, A., and Fundele, R. (2004).

Loss-of-imprinting of Peg1 in mouse interspecies hybrids is correlated with altered growth. Genesis *39*, 65–72.

Shi, W., Krella, A., Orth, A., Yu, Y., and Fundele, R. (2005). Widespread disruption of genomic imprinting in adult interspecies mouse (Mus) hybrids. Genesis *43*, 100–108.

Shoshani, O., Massalha, H., Shani, N., Kagan, S., Ravid, O., Madar, S., Trakhtenbrot, L., Leshkowitz, D., Rechavi, G., and Zipori, D. (2012). Polyploidization of murine mesenchymal cells is associated with suppression of the long noncoding RNA H19 and reduced tumorigenicity. Cancer Res. *72*, 6403–6413.

Spandidos, A., Wang, X., Wang, H., Dragnev, S., Thurber, T., and Seed, B. (2008). A comprehensive collection of experimentally validated primers for Polymerase Chain Reaction quantitation of murine transcript abundance. BMC Genomics *9*, 633.

Spandidos, A., Wang, X., Wang, H., and Seed, B. (2010). PrimerBank: a resource of human and mouse PCR primer pairs for gene expression detection and quantification. Nucleic Acids Res. *38*, D792–D799.

Sun, S., Noviski, A., and Yu, X. (2013). MethyQA: a pipeline for bisulfite-treated methylation sequencing quality assessment. BMC Bioinformatics *14*, 259.

Tamura, K., G. Stecher, D. Peterson, A. Filipski, and S. Kumar. (2013). MEGA6: Molecular evolutionary genetics analysis version 6.0. Mol. Biol. Evol. *30*, 2725–2729.

Tilghman, S.M. (1999). The Sins of the Fathers and Mothers: Genomic Imprinting in Mammalian Development. Cell *96*, 185–193.

Tukey, J.W. (1949). Comparing Individual Means in the Analysis of Variance. Biometrics *5*, 99–114.

Turner, L.M., Schwahn, D.J., and Harr, B. (2012). Reduced Male Fertility Is Common but Highly Variable in Form and Severity in a Natural House Mouse Hybrid Zone. Evolution *66*, 443–458.

Tycko, B., and Morison, I.M. (2002). Physiological functions of imprinted genes. J. Cell. Physiol. *192*, 245–258.

Varrault, A., Gueydan, C., Delalbre, A., Bellmann, A., Houssami, S., Aknin, C., Severac, D., Chotard, L., Kahli, M., Le Digarcher, A., et al. (2006). Zac1 Regulates an Imprinted Gene Network Critically Involved in the Control of Embryonic Growth. Dev. Cell *11*, 711–722.

Virani, S., Colacino, J.A., Kim, J.H., and Rozek, L.S. (2012). Cancer Epigenetics: A Brief Review. ILAR J. *53*, 359–369.

Vrana, P.B., Guan, X.J., Ingram, R.S., and Tilghman, S.M. (1998). Genomic imprinting is disrupted in interspecific Peromyscus hybrids. Nat. Genet. *20*, 362–365.

Vrana, P.B., Fossella, J.A., Matteson, P., del Rio, T., O'Neill, M.J., and Tilghman, S.M. (2000). Genetic and epigenetic incompatibilities underlie hybrid dysgenesis in Peromyscus. Nat. Genet. *25*, 120–124.

Wang, X., and Seed, B. (2003). A PCR primer bank for quantitative gene expression analysis. Nucleic Acids Res. *31*, e154–e154.

Wang, X., Sun, Q., McGrath, S.D., Mardis, E.R., Soloway, P.D., and Clark, A.G. (2008). Transcriptome-wide identification of novel imprinted genes in neonatal mouse brain. PLoS ONE *3*, e3839.

Wang, X., Soloway, P.D., and Clark, A.G. (2011). A Survey for Novel Imprinted Genes in the Mouse Placenta by mRNA-seq. Genetics *189*, 109–122.

Wood, A.J., Roberts, R.G., Monk, D., Moore, G.E., Schulz, R., and Oakey, R.J. (2007). A screen for retrotransposed imprinted genes reveals an association between X chromosome homology and maternal germ-line methylation. PLoS Genet. *3*, e20.

Wolf, J.B., and Hager, R. (2006). A maternal-offspring coadaptation theory for the evolution of genomic imprinting. PLoS Biol. *4*, e380.

Wutz, A., Smrzka, O.W., and Barlow, D.P. (1998). Making sense of imprinting the mouse and human IGF2R loci. Novartis Found. Symp. *214*, 251–259; discussion 260–263.

Wutz, A., Smrzka, O.W., Schweifer, N., Schellander, K., and al, et (1997). Imprinted expression of the Igf2r gene depends on an intronic CpG island. Nature *389*, 745–749.

Xu, Y.Q., Goodyer, C.G., Deal, C., and Polychronakos, C. (1993). Functional Polymorphism in the Parental Imprinting of the Human IGF2R Gene. Biochem. Biophys. Res. Commun. *197*, 747–754.

APPENDIX A

Unsuccessful Primer Sets

Table 15. Primers used Unsuccessfully in PCR to Amplify Bisulfite-Modified DNA. A description of the primers that were used unsuccessfully in PCR. The name of the primers, the name of the gene associated with the primers, and the primer sequences are listed here. The annealing temperatures that were attempted with each primer set are also listed. The primer sequences were obtained from WAMIDEX (Schulz et al., 2008). The symbol "Bi" indicates that the particular primer was associated with bisulfite-modified template and amplified the DMD associated with the gene.

Gene	Primer Name	Primer Sequence	Annealing Temperature
Grb10	Grb10-Bi-1-F	GAGAAGATATGTTGAAGTTATGGTG	46°C
	Grb10-Bi-1-R	TAAATACAATTACTACTTATTACATAATATC	
Grb10	Grb10-Bi-4-F	GAGTTYGTAGGAGTTGTTTATTATTTGGATTATTGTAG	46°C and 51°C
	Grb10-Bi-4-R	AATTCRAAAACTATCCACTAACCCC	
Gtl2-Dlk1	Gtl2-Dlk1-Bi-1-F	ATTTAYGGTATATGAGTTTTATTATTTTGTATGTG	46°C, 51°C, and 52°C
	Gtl2-Dlk1-Bi-1-R	TAATCCATAACRAACCTTAACACCAATCCATAAC	
Mcts2	Mcts2-Bi-2-F	TTTTTAAGTATTAGAATATTGGGGGATT	51°C
	Mcts2-Bi-2-R	AACATAATCTTAATAAAAAAACACC	
Nap1l5	Nap1l5-Bi-2-F	TTTGGAATTTTTTGTTAAATTTGGT	49°C
	Nap1l5-Bi-1-R	CACAACTACAAAACCTCTCTAAACC	

Table 16. Primers used Unsuccessfully in Real-Time PCR. A description of the primers that were used unsuccessfully in real-time PCR. The name of the primers, the name of the gene associated with the primers, and the primer sequences are listed here. The primer sequences were obtained from PrimerBank and IDT PrimeTime® (PrimeTime® program, 2015; Spandidos et al., 2008, 2010; Wang and Seed, 2003).

Gene	Primer Name	Primer Sequence
Gapdh	Gapdh F1	AATGGATTTGGACGCATTGGT
	Gapdh R1	TTTGCACTGGTACGTGTTGAT
Gapdh	Gapdh F2	AGCTTCGGCACATATTTCATCTG
	Gapdh R2	CGTTCACTCCCATGACAAACA
Gapdh	Gapdh-3F	TTGTCATGGGAGTGAACGAGA
	Gapdh-3R	CAGGCAGTTGGTGGTACAGG
Gpr1-Zdbf2	Zdbf2 F1	ACTCTGATGGAACGCTTTTTGC
	Zdbf2 R1	ACCACCACCACTTCAGGTGA
Gpr1-Zdbf2	Zdbf2-PB-2F	ACTCTGATGGAACGCTTTTTGC
	Zdbf2-PB-2R	TCTGGCTCATTTGGTGCAGAT
Grb10	Mm.PT.58.31223576	TGCGATAGTTTTGGTACAGGAG
		AAGCGAAGACCGAGATGAAG
Grb10	Grb10-PB-1F	GTGGTGGAGATTCTAACCGACA
	Grb10-PB-1R	ACCTCTCTAATCCCAGTTGTGG
Grb10	Grb10-PB-2-F	CCTGCCAAGCATGATGTCAAA
	Grb10-PB-2-R	CCAGGCACCTCTCTAATCCCA
Grb10	Grb10-PB-3-F	ACCATGAGATCGTGGTCCAAG
	Grb10-PB-3-R	TTGCGTCCTACCTCTTTCACC
Igf2r	Igf2r F1	ATTAAGCCACGGCTCGATACC
	Igf2r R1	TTCTCAAAAGTGAGTCACCCAC
Igf2r	Igf2r-PB-2F	TGCCAGCCTTCAGATTCACAG
	Igf2r-PB-2R	CAGATAGCCACCATTTAGCTTGA
Igf2r	Igf2r-4-F	GGGAAGCTGTTGACTCCAAAA

	Igf2r-4-R	GCAGCCCATAGTGGTGTTGAA
Mest	Mest F1	AGAGTGGTGGGTCCAAGTAGG
	Mest R1	AAGCACAACTATCTCAGGGCT
Mest	Mest-PB-2F	TGACCCTGAGGTTCCATCGAG
	Mest-PB-2R	GCCGCAGAAGGGACTCTAC
Mest	Mest-3-F	CTCCAGAACCGCAGAATCAAC
	Mest-3-R	AGATACCTCCATTCGACAGACAG
Mest	Mest-4-F	GTGGTGGGTCCAAGTAGGG
	Mest-4-R	AAGCACAACTATCTCAGGGCT
Mest	Mm.PT.58.12987460	CCAGATCTTGTACCAGTCATAGC
		GCCTACGCATCTTCTACCAAG
Nap1l5	Nap1l5 F1	GCCGAGGACGAGGTAATGG
	Nap1l5 R1	CATTTCACGGAATTGGGCAAG
Nap1l5	Nap1l5-IDT-F	CTGGAGAAGAAGTACAACGATATCTA
	Nap1l5-IDT-R	CCTCTTCCTCGTCATCTTCATC
Nckap1 or H19	Mm.PT.58.12289852	GTGATCTGCAAGGCTAAGTGA
		CATGACCTCCCTAAGTGTGAAG
Peg10	Mm.PT.58.12887449	CTCGTGGTTGGCGTCTT
		CTCATCCTTCGTGGCATCG
Peg10	Peg10-PB-1F	TGCTTGCACAGAGCTACAGTC
	Peg10-PB-1R	AGTTTGGGATAGGGGCTGCT
Peg10	Peg10-PB-2-F	CCTGAGAAGTTCGATGGCAAC
	Peg10-PB-2-R	CGGATGCGGTCAACTGAGAA
Peg10	Peg10-PB-3-F	GCTACTGCCAAGCTGCAAAG
	Peg10-PB-3-R	CTGGGCAATCATCTGGAATGC
Zac1	Zac1 F1	ATGGCTCCATTCCGCTGTC
	Zac1 R1	CTCAGCCTTCGAGCACTTGAA
Zac1	Zac1-PB-2F	CAAAGCCTTCGTCTCCAAGTAT
	Zac1-PB-2R	GTCCTTCCGGTTGAATGTCTT
Zac1	Zac1-4-F	ACCTCCAGACCCACGATCC

	Zac1-4-R	CCAGCATGGTGTGGTACTTCT
Zim2	Zim2 F1	CCTCTCAAGGCTGATGTTAGTG
	Zim2 R1	ATTTGCCCTCATGGAGCTATAC
Zim2	Zim2-2F	GGATTGGAGGAGGAGGAGTTA
	Zim2-2R	CCAGGAATCAGGTCACGTTTAG